DEVELOPMENT OF A FLIGHT ENVELOPE PROTECTION SYSTEM FOR A HELICOPTER IN AUTOROTATION

OTOROTASYON DURUMUNDA BİR HELİKOPTER İÇİN UÇUŞ ZARFI KORUMA SİSTEMİ GELİŞTİRİLMESİ

EZGİ SELİN ÇUVALCI

DOÇ. DR. S. ÇAĞLAR BAŞLAMIŞLI

Supervisor

Submitted to

Graduate School of Science and Engineering of Hacettepe University

as a Partial Fulfillment to the Requirements

for the Award of the Degree of Master of Science

in Mechanical Engineering

2021

for my grandmother, Ayşe

ABSTRACT

DEVELOPMENT OF A FLIGHT ENVELOPE PROTECTION SYSTEM FOR A HELICOPTER IN AUTOROTATION

Ezgi Selin ÇUVALCI

Master of Science, Department of Mechanical Engineering

Supervisor: Assoc. Prof. Dr. S. Çağlar BAŞLAMIŞLI

Co-Supervisor: Assoc. Prof. Dr. İlkay YAVRUCUK

January 2021, 72 pages

In this thesis, a flight envelope protection system was developed for a helicopter in autorotation to prevent main rotor speed limit exceedance. A rotor speed estimation model was developed using a neural network based algorithm for a helicopter at autorotation. Using the lead estimate, the collective input margin and pitch angle margin are calculated. Two flight envelope protection methodologies were proposed using these margins. The envelope protection strategies were shown through simulations to be successful in preventing the rotor speed limit exceedance.

Keywords: Flight envelope protection, autorotation, rotor speed estimation, control margin, limit margin

ÖZET

OTOROTASYON DURUMUNDA BİR HELİKOPTER İÇİN UÇUŞ ZARFI KORUMA SİSTEMİ GELİŞTİRİLMESİ

Ezgi Selin ÇUVALCI

Yüksek Lisans, Makine Mühendisliği Bölümü

Tez Danışmanı: Doç. Dr. S. Çağlar Başlamışlı

Eş Danışman: Doç. Dr. İlkay Yavrucuk

Ocak 2021, 72 Sayfa

Bu tezde otorotasyonda ana rotor hızının limitleri aşmaması için bir uçuş zarfı koruma sistemi geliştirilmiştir. Otorotasyon manevrası sırasında ana rotor hızı tahmini için yapay sinir ağı algoritması geliştirilmiştir. Hesaplanan bu ön tahmin kullanılarak helikopterin hatve açısı ve kolektif kontrolü için limit ve kontrol marjinleri hesaplanmıştır. Bu iki marjin kullanılarak iki uçuş zarfı kontrol metodu önerilmiştir. Oluşturulan uçuş zarfı koruma sistemleri ile uçuş simülasyonları gerçekleştirilmiş ve otorotasyon manevrası sırasında rotor hızının limit dışına çıkmasının engellendiği gösterilmiştir.

Anahtar Kelimeler: uçus zarfı koruma, otorotasyon, limit belirleme, kontrol marjin

ACKNOWLEDGEMENTS

I would like to express my gratitude to my supervisor Assoc. Prof. Dr. S. Çağlar BAŞLAMIŞLI and my co-supervisor Assoc. Prof. Dr. İlkay YAVRUCUK for their guidance and advice throughout this study.

I would also like to express my deepest gratitude to Dr. Gönenç GÜRSOY for his encouragement, guidance, and criticism for my academic and also my professional studies. I would like to thank him for creating a great team in Aerotim Engineering, and for his hard work and enthusiasm for engineering; which provided a baseline for me to build my studies upon.

My deepest heartfelt appreciation goes to my husband Ufuk for his enduring love, support, intellectual guidance, wisdom, and most of all his friendship.

I would like to offer my special thanks to my friends for their support for this thesis to finish: especially to N. Ece Ataoğlu and Tuğçe N. Pekçetin for emotional support, cheer, and encouragement whenever I felt it was never going to end; to Yiğit Vural for making me apply to the graduate program and being my classmate; to Asya&Sonat Çelebi for all the cheer during the quarantine; and all others for helping me throughout this period.

I am deeply thankful to my family: my brother Ozan, my mother Sevinç, and my father Seyfettin for their endless love and support from the very first day of my life. Additional thanks to my little brother Ozan for completing his master's degree before me, and sharing his experiences on writing the thesis which eased my way when the time was against me. Finally, I would like to thank my grandmother Ayşe Bakoğlu, who always wanted the women in our family to be well educated and independent.

Ezgi Selin ÇUVALCI

February 2021, Ankara

TABLE OF CONTENTS

LIST OF FIGURES

NOMENCLATURE

α	Tip path plane angle
β_0	Rotor coning angle
β_{1c}	Pitch angle of the tip-path plane
β_{1s}	Roll angle of the tip-path plane
β_m	Mast angle
g	Gravity
J	Inertia
Ω	Rotational speed of the rotor
ϕ, θ, ψ	the Euler rotations defining the orientation of the helicopter
ψ_b	Blade azimuth
Q_e	Engine torque
Q_p	Shaft torque of the power turbine
m	Aircraft mass
ρ	Air density
p, q, r	Angular velocities
r_b:	Blade radial location
R	Rotor radius
σ_{coll}	Collective stick input
σ_{long}	Longitudinal cyclic input
T	Thrust
θ_0	Rotor blade collective pitch angle
θ_{1c}, θ_{1s}	Rotor blade cyclic pitch angles
$\dot{\theta}_e$	Engine speed

$\dot{\theta}_x$	Transmission speed
$\acute{\mu}$, $\acute{\eta}$	Non-dimensional horizontal and vertical airspeeds
u, v, w	Linear velocities
V	Air velocity
V'	Net air velocity
$V_{xhub}, V_{yhub}, V_{zhub}$	Local hub velocities
w_w	Inflow (induced velocity)
w_{w_0}	Inflow (induced velocity) at hover condition
$\acute{w}$	Non-dimensional induced velocity

Subscripts

FUS	Fuselage
HT	Horizontal Tail
VT	Vertical Tail
e	Engine
$pred$	Predicted

Abbreviations

AAIB	Air Accidents Investigation Branch
AFCS	Automatic Flight Control System
CG	Center of Gravity
CP	Center of Pressure
DOF	Degree of Freedom
EPS	Envelope Protection System
FBW	Fly-By-Wire

NN	Neural Network
PNN	Polynomial Neural Network
SAS	Stability Augmentation System
VRS	Vortex Ring State

1. INTRODUCTION

1.1.Problem Definition and General Information

Helicopter autorotation is an extremely hard flight condition to control. Fatal accidents may occur due to loss of control during the autorotative flight. It is crucial to keep the helicopter inside the operational flight envelope to ensure safety. During autorotation, one of the most important limitations is the rotor speed boundaries. The pilot should keep the rotor rpm between the maximum and minimum rpm limits. Very high rotor speeds might cause structural damage, whereas very low rotor speeds might cause loss of lift force, or loss of control, leading to fatal accidents.

In this study, the helicopter rotor speed is estimated during autorotation, control, and limit margins are calculated, then these margins are cued to the pilot to prevent flight envelope limit exceedance. A helicopter simulation model was developed and used in this thesis. The helicopter model is based on high fidelity modeling methods that were developed in Aerotim Engineering LLC where the author is currently employed.

During the author's work in Aerotim, the autorotative flight was deeply discussed with several helicopter pilots. Most of the pilots claimed that during autorotation, the control of rotor speed is performed using the collective inputs and changing the helicopter pitch attitude. This implied that the rotor speed was a fast responsive state in response to a change in pitch angle, and to a given collective input. All further studies were based on this assumption. The rotor speed response to given inputs or change in parameters was investigated using a simulation model. It was verified that the pitch angle and collective input were the main parameters to control the rotor speed. Based on this assumption, the rotor speed was modeled using a neural network algorithm that uses the collective control input, pitch angle, and local hub velocities as inputs to the rotor rpm model. The network was trained offline with a dynamic trim database of autorotative flight conditions. The database was generated offline using the developed helicopter model.

This rotor speed estimation network was used to calculate the available collective input control margin and the available pitch angle limit margin. These margins can be used in piloted flight to cue the pilot for a safe flight during autorotation. In this study, a mathematical pilot model was developed. The pilot model was used to avoid the envelope limits during autorotative flight. The results showed that the rotor rpm limit avoidance was successful with the developed algorithm.

1.2.Literature Survey

1.2.1. Helicopter Control System

Generating the lift, providing propulsion, and achieving stability in a helicopter are all accomplished mainly by the rotor system. The major control inputs in a helicopter are the collective pitch for vertical motion, tail rotor pitch for directional motion, and cyclic pitch for longitudinal and lateral motion. An illustration of the main helicopter flight controls is shown in Figure 1.2.1.

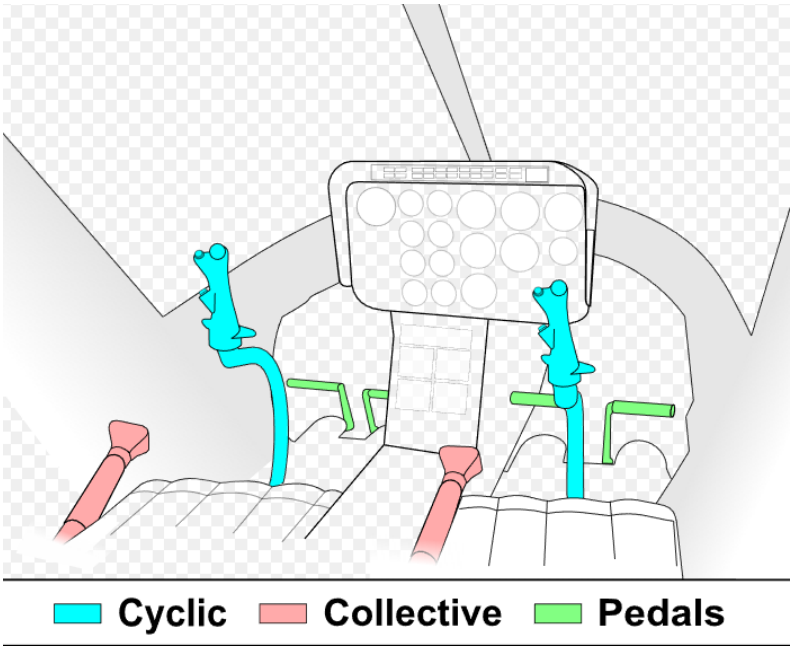

Figure 1.2.1 Illustration of helicopter flight controls [1]

The collective input applies the same amount of pitch angle change to all blades of the rotor, and it is used for the direct control of the vertical thrust (lift force). This change in

blade pitch is applied through a series of linkages. The collective stick, also called a collective lever, has one degree of freedom. It can be pushed or pulled up and down. Figure 1.2.2 shows an example of the collective input and the corresponding rotor blade position.

Figure 1.2.2 Collective position and corresponding blade pitch angle [2]

When the blade pitch angle is changed, the angle of attack hence the generated forces on the blades are also changed. By increasing the collective input, the lift and drag forces are also increased on the blade.

The increase of blade drag causes the angular rotor speed (also called rotor rpm) to decrease. During the flight, a constant rotor rpm should be maintained for the stability of the flight. To maintain a constant rotor rpm, different mechanisms exists in different helicopters. The correlator and/or governor systems in the helicopters adjust the engine power automatically during a powered flight to maintain the rotor rpm constant. When these systems are not enough or when they do not exist in the helicopter, the pilot has to regulate the rotor rpm using the throttle. The throttle also adjusts the engine power, same as the correlator/governor systems but operates manually.

The cyclic pitch control, or the cyclic stick, is shown in Figure 1.2.3. The pilot input to the cyclic causes the rotor to tilt longitudinally or laterally according to the cyclic input direction. This is done by changing the blade pitch angle to different values at different azimuths during the cycle of rotation. As a result, the resultant lift force direction is also tilted, developing a propulsive force for the helicopter. This input will also give a moment about the center of gravity hence pitch or roll motion will occur.

Figure 1.2.3 Cyclic stick inside the cockpit [2]

The pedal inputs also called anti-torque pedals, controls the blade pitch angles of the tail rotor. Figure 1.2.4 shows the anti-torque pedals.

Figure 1.2.4 The anti-torque pedals [2]

The tail rotor is used mainly to overcome the torque effect of the main rotor. During the flight, the torque varies with the changes in power used by the main rotor. Hence the tail rotor thrust must be adjusted accordingly. The pedals are also used to control the heading of the helicopter in hover. Figure 1.2.5 shows a schematic representation of the main rotor torque and tail rotor anti-torque.

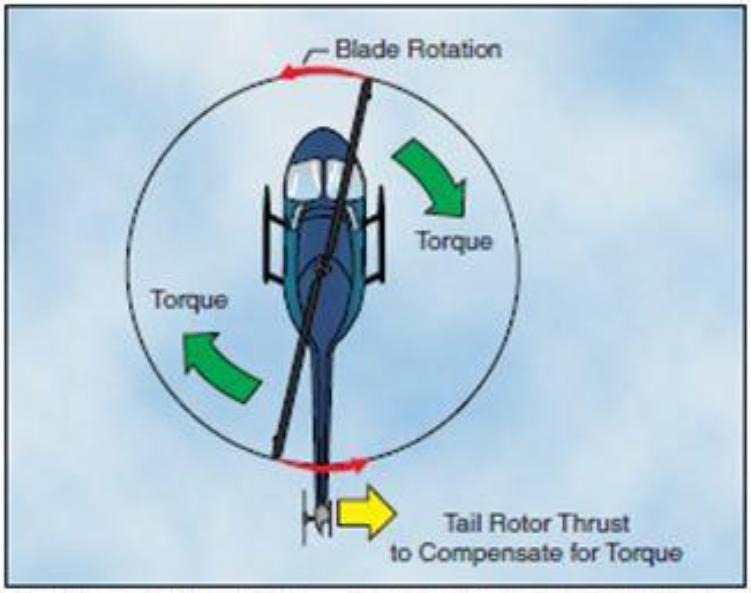

Figure 1.2.5 Illustration of torque compensation [2]

The control inputs given from collective, cyclic, and pedals are linked to the main rotor and tail rotor blades through mechanical, hydraulic, or electrical linkages. The inputs that are given through cyclic and collective sticks are linked to main rotor blades usually with a swashplate. The conventional swashplate structure is shown in Figure 1.2.1. The cyclic input is transmitted with a more complex mechanism than the collective pitch. The swashplate is tilted as the rotor rotates and a lift difference is generated through the rotor disk by changing the blade pitch angles at different azimuths.

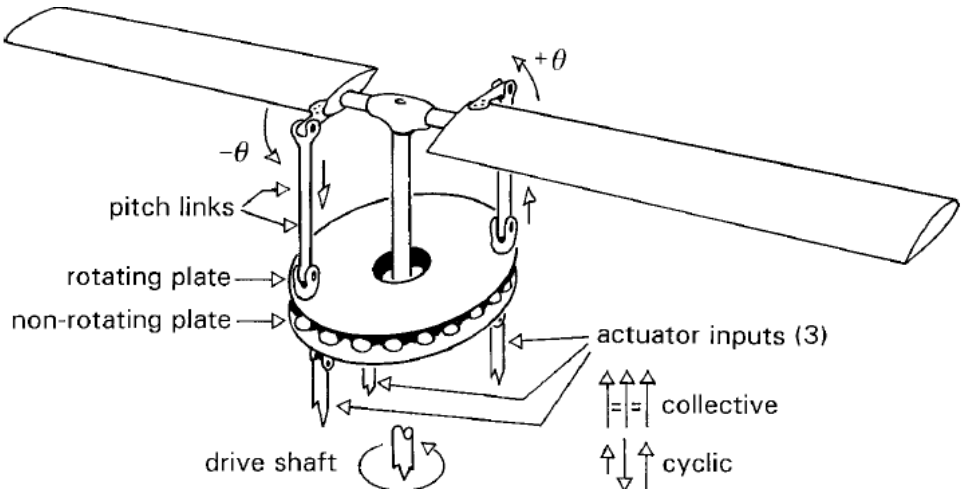

Figure 1.2. 6 Rotor control through a swashplate[3]

Some axis systems are mentioned throughout the thesis to explain the calculations. The body axes are shown in Figure 1.2.7. The origin is at the center of gravity, and the axes are formed in a right-handed system. The x-axis is in the plane of symmetry pointing forward. The y axis points right, and the z-axis points down.

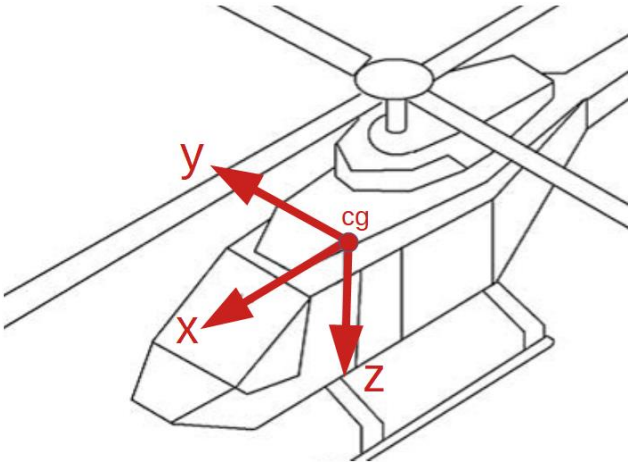

Figure 1.2.7 Helicopter body axes

Another axis system mentioned in the thesis is the local element axes. The origins of these axes are the reference points that the forces and moments of the component are acting on. The individual element local axes are displaced from the body axes origin by a position vector. Figure 1.2.8 shows the local hub axes.

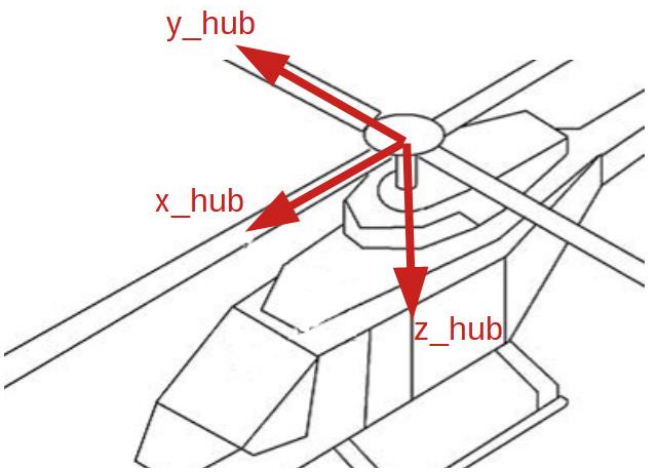

Figure 1.2.8 Local hub axes

1.2.2. Autorotation

When a failure occurs in the drive train or an engine, or in a situation where tail rotor control is lost, the helicopter should be entered to autorotative flight. In the absence of torque applied by the engine, the rotation of the rotor is provided with the airflow through the rotor disk as the helicopter descends.

After the engine failure, the pilot should lower the collective immediately, and set the controls to the proposed positions as in the helicopter flight manual.[3] If the collective is not decreased, the blade drag will be too high to overcome, and since the engine power is lost the rotor rpm will drop too much. The flow around the blade will be disrupted and a blade stall will occur. The lift force will be lost, the helicopter will fall with a high descent rate, the control will be lost. Hence, the pilot quickly lowers the collective after the engine failure and stops the rotor rpm decrease. The blade pitch angles will decrease and the drag and lift forces will also decrease. The helicopter will start to descend. The air will flow up through the rotor disk. The rotation of the rotor will be provided by the airflow, not by the engine power. The rotor speed increases again.

Helicopters have a clutch mechanism that is used to disengage the transmission from the rotor. In normal operating conditions, such as powered flight, the engine speed is greater

than the rotor speed. The transmission is engaged to the rotor, hence transmits this rotation to the rotor. When the rotor speed is greater than the engine speed, the clutch mechanism disengages the transmission from the rotor.

This will cause the rotor to act like a windmill, which is called autorotation.[4] In an autorotative state, the direction of airflow through the rotor disk is the opposite of normal (powered) flight. Figure 1.2.9 shows the direction of airflow through the rotor disk for these two cases: powered forward flight and forward flight in autorotation.

The potential energy that the helicopter has is used for the rotation of the rotor as the helicopter descends. When the rotor speed is gained again, the generated lift force is used for the deceleration of vertical speed. The autorotation is not an uncontrollable flight condition. Apart from the engine, the helicopter controls are still in use if there is no other damage or failure in the helicopter's systems. But of course, the sensitivities, performance, and maneuvering capabilities of the helicopter is less than a powered flight condition. Level flight in autorotation can not be performed since the engine does not supply any power to overcome gravity. The pilot can fly the helicopter to a safe landing site if the height of the helicopter is high enough.

To keep the rotor speed at reasonable values, the pilot uses the helicopter pitch angle and collective blade pitch. High rotor speed can cause structural problems whereas low rotor speed can cause stall on the rotor blades; the lift force would be lost and the helicopter would crash.

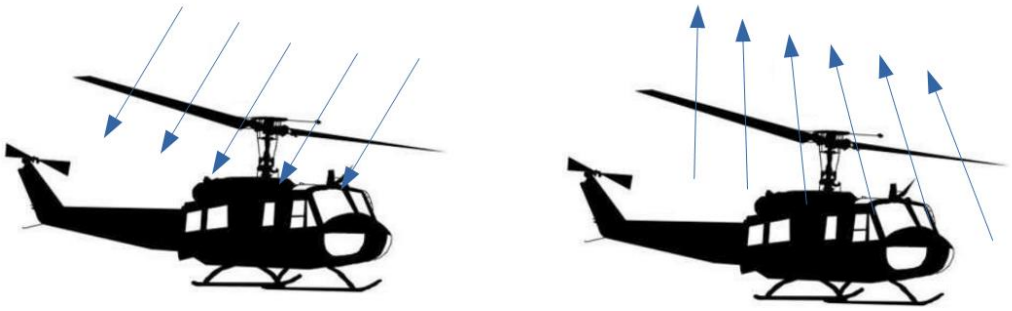

Figure 1.2.9. Airflow direction in powered flight (Left) and autorotation (Right)

The effect of collective input on rotor speed can be simplified as; by lowering the collective pitch of the blades, the overall blade drag is reduced, and the rotor speed increases. When the collective pitch is increased, the drag also increases, resulting in a decrease in rotor speed.

The pitch attitude of the helicopter also affects the rotor speed during autorotation. When the pilot gives a backward longitudinal cyclic input, the helicopter performs a nose up maneuver. This will increase the amount of air flowing through the rotor disk, and the rotor speed increases. Similarly, when the helicopter pitches down, the airflow is reduced, and the rotor speed is decreased.

This is a very simple explanation of the overall response but in reality, it is not a simple linear relation. It is highly coupled and nonlinear, and hard to control since these given inputs do not only affect the rotor speed but all of the helicopter motion. Lowering the collective increases the rotor rpm, but it also decreases the overall generated thrust. Thus, the propulsive force is also decreased. The helicopter forward speed is decreased and this causes the airflow through the disk to decrease, which also decreases the rotor rpm. But at the same time, since the lift force is also decreased, the helicopter starts to descend at a higher rate, which again increases the amount of airflow through the disk. To prevent the high descend rate, the pilot will pull the longitudinal cyclic and increase the helicopter pitch angle, this also affects the rotor rpm. In brief, the rotor rpm behavior is highly coupled and nonlinear.

1.2.3. Flight Envelope Protection Systems

Aircraft have several performance limitations that should not be exceeded to prevent an unwanted decrease in overall flight safety and control authority.[5] These limitations are generally aerodynamic, structural, power, and control related. The overall limitations define the boundaries of safe flight conditions, under which the aircraft can fly safely without a significant risk of failure. As an example, the V-n diagram shows the aerodynamic and structural limitations. It defines the range of the angle of attack, airspeed, and the normal load factor that the aircraft should not exceed. The limits can be defined at normal operation, at maneuvering flight, or in gust conditions. Figure 1.2.10 is an example of a basic flight envelope diagram for an aircraft. There are also limitations related to the power system such as maximum engine torque. These limitations are combined together with the general term 'flight envelope'.

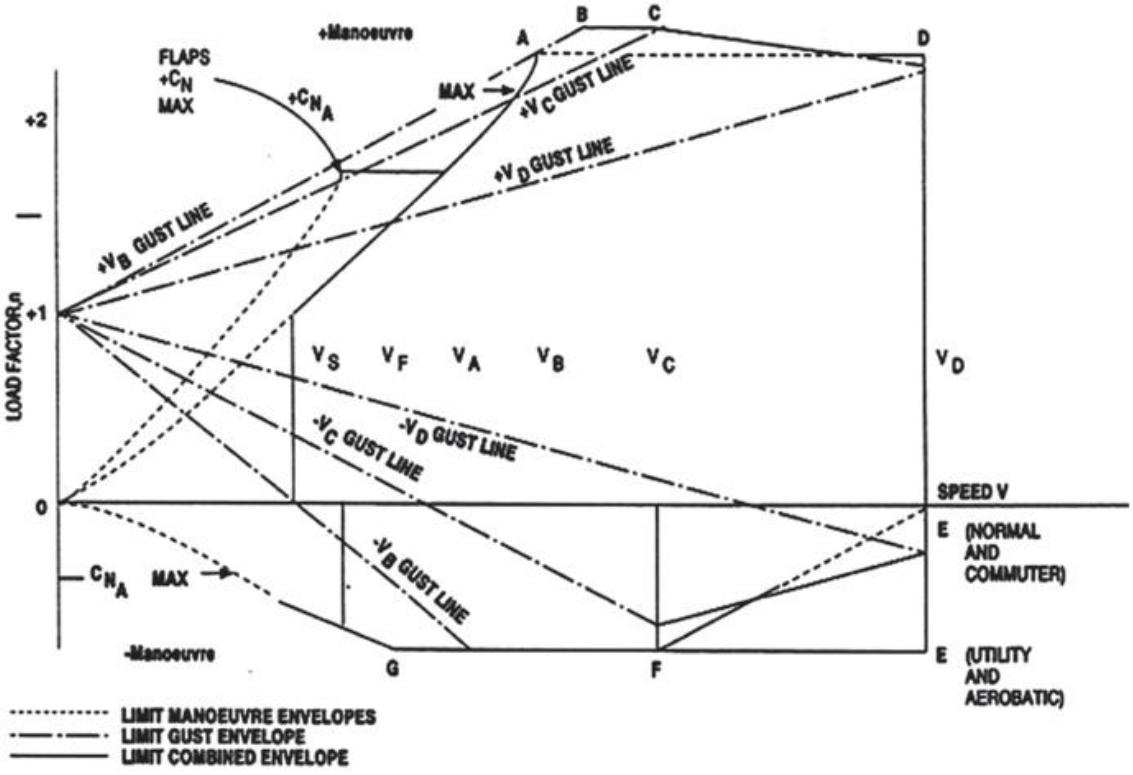

Figure 1.2.10. Typical basic flight envelope diagram of CS-23[5]

As discussed before, the pilot has to monitor all the limits through the indicators during the flight which increases the workload. The research on flight envelope protection systems (EPS) aims to decrease this workload by cueing the pilots during flight through visuals or other equipment. These systems focus on increasing safety in both piloted and autonomous flights.

During the flight, the pilots avoid getting too close to flight envelope limits, so the operating flight envelope is narrower than the actual aircraft capability. The envelope protection systems help to use the aircraft with full capacity performance while ensuring the safety of the flight.

There are several methods used for envelope protection during piloted flight. The pilot can be warned using aural warnings, as well as visual cues on the displays of the cockpit, or by creating a vibration on the controls as the aircraft approaches the limits. These cues should be sent to the pilot before the aircraft reaches the limit so that there will be enough time to prevent the limit exceedance. An example of the aural and visual cues can be found in the RAH-66 helicopter. The designed cueing system aims to increase the safety and awareness of the pilot. Structural and power-related limit cues are given to the pilot through the Helmet Mounted Display as visual cues, and as aural cues through the headset[6]. In another study, situational awareness was be provided to the pilot through developed displays that inform the state of the aircraft during flight. The cueing was performed using visual cues.[7]

Flying a helicopter is rather a hard mission to accomplish. The pilots' every input, using their hands and feet, are engaged with the vehicle dynamics. The automatic flight control systems (AFCS) are developed to decrease the pilot's workload. This decrease in the workload is valuable in the sense that, the pilots do not only fly the helicopter, but they also have to accomplish several tasks. These tasks could be transferring a load, doing emergency missions, carrying a patient to a hospital, putting out fires, etc. If the pilot is very busy concentrating on flying, it becomes harder to fulfill the other required tasks. For this reason, the developments in the automatic control systems are towards reducing

the pilot workload. The improvements in Automatic Flight Control Systems (AFCS) enabled another method for flight envelope protection. Using AFCS or Stability Augmentation Systems (SAS), the pilot inputs can be modified to keep the aircraft within the boundaries of the flight envelope.

Modern aircraft usually have fly-by-wire (FBW) control systems, in which the controls are not mechanically linked to the control surfaces of the aircraft. The control stick that the pilot holds is not a simple stick. These sticks also simulate the mechanical loads of the control cyclic, while digitally transferring the given control inputs to the aircraft. This system enables another EPS method. The FBW system can be used to warn the pilot, for example by shaking the control cyclic. This is called tactile cueing. In [8], the collective control margin was calculated for continuous torque limits during non-emergency flight. It is shown with pilot testing that collective tactile cueing during flight is useful in reducing the pilot work-load. The study also concludes that workload decrease directly impacts the performance and accuracy of the task. In another study [9], the active sidestick and conventional inceptors were compared for tactile cueing. The same tasks were performed in piloted simulations, and the methods were compared. Almost an equivalent performance was achieved with both systems.

The tactile cues provide hard stops and soft stops for the cueing of limits. The hard stops are used for limits that should never be exceeded during flight, for example, a maximum load factor for a fixed-wing aircraft. On the other hand, soft stops are used for the limit parameters that are less-destructive after a limit exceedance and has still a little more tolerance. These hard and soft stops limit the control cyclic motion with force feedbacks that are hard or soft, according to the limiting parameter.

A significant lead estimation of the limit parameter is required to ensure the limits are avoided in tactile cueing. It has been shown that the Polynomial Neural Networks (PNN) was effective in providing the necessary lead estimate of the limit parameter[10].

Another study used tactile cueing for flight envelope protection to avoid the Vortex Ring State (VRS) [11]. The study showed the cue allowed the pilots to rapidly reach a sink rate that would prevent exceeding the safe limits. Several other methodologies were also investigated and found effective in-flight envelope protection in small-scale aircrafts such as PID-based control limiting approach, command limiting approach, constrained flight control law approach, and virtual control limiting approach[12].

The state or the parameter that defines the boundary of a flight envelope is called the limit parameter in the terminology. Some examples of limit parameters can be listed as the normal load factor, airspeed, angle of attack, engine speed, continuous torque, etc. It is important to understand the behavior of the limit parameter in order to develop an effective envelope protection system. Understanding the response shape of the limit parameter to the changes of the states or inputs is crucial to decide on the limit avoidance method. Depending on their response types, the limit parameters can be classified as peak response critical, steady-state critical, peak and steady-state critical, and integral response critical.[13]

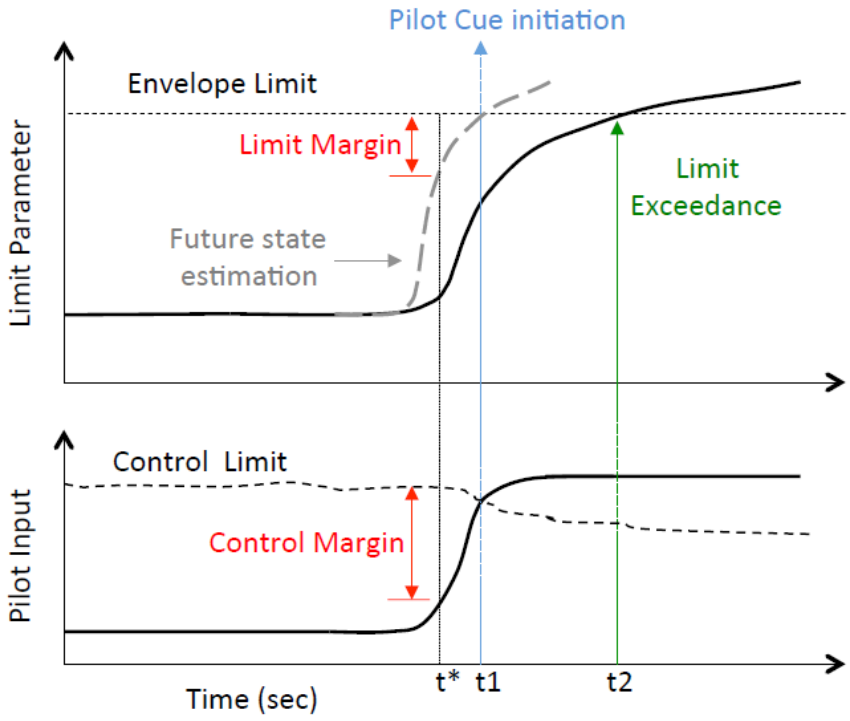

Figure 1.2.11 Limit Detection [13]

As previously mentioned, a lead estimation is required for limit avoidance. The proximity of a limit parameter should be estimated, which is called the limit margin. This is the margin that the state can travel before reaching the limit value. If a limit is required to be defined on a control input, the margin should be transferred to the controls, which is called the control margin. The prediction of these margins is called limit detection. Figure 1.2.11 shows a schematic representation of the limit detection process[13]. Control input and the corresponding response of a limit parameter is shown in the figure. The predicted limit and control margins are also shown. It was mentioned before that the margin estimations require estimation of the corresponding future state, which is a lead-time estimation. The point where the future state is detected to reach the envelope boundary, the margin is zero, and the cueing of the pilot is initiated.

In [8], a collective cueing system was developed. The system cues the pilot to a variety of envelope limits of transient and continuous transmission torque limits, and the optimal rpm following an engine failure emergency. The cueing system uses a neural network algorithm to predict the collective control margin due to torque limit during powered flight. For autorotation, the optimal rpm is assumed and the corresponding collective input was estimated. This collective control is cued to the pilot to follow during an engine inoperative emergency. This study does not provide information about collective margins during autorotation to avoid rpm limits, rather it suggests a control input sequence to stay at an optimum rpm. In [14], a flight envelope protection system for a tiltrotor aircraft was also developed by the same authors. This study developed the basis of the previously mentioned study on collective cueing. Figure 1.2.12 and 1.2.13 show the results of the study on tilt-rotor aircraft. This study concludes that using neural networks for the calculation of the dynamic trim response of the limit parameters provides an efficient lead estimation so that limit exceedance can be prevented by cueing or by using automatic flight control systems.

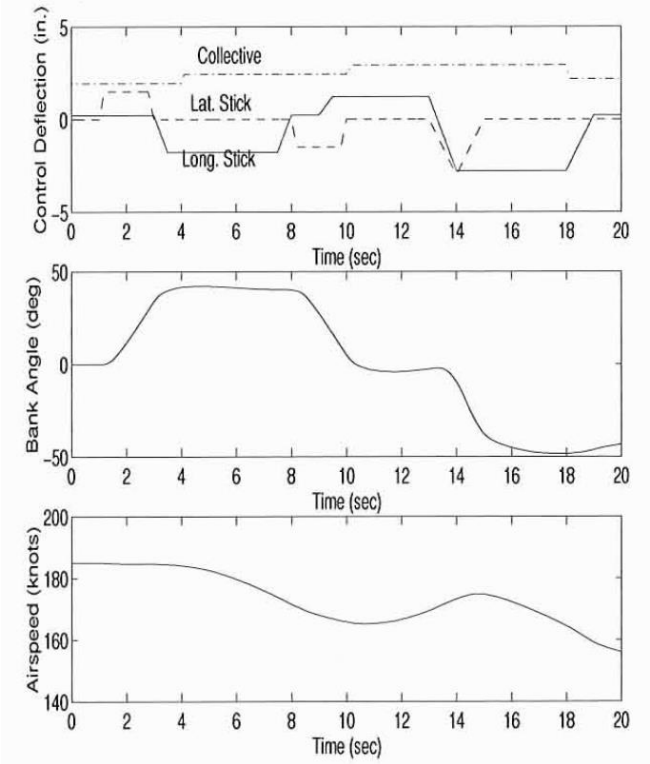

Figure 1.2.12 Sample test maneuver [14]

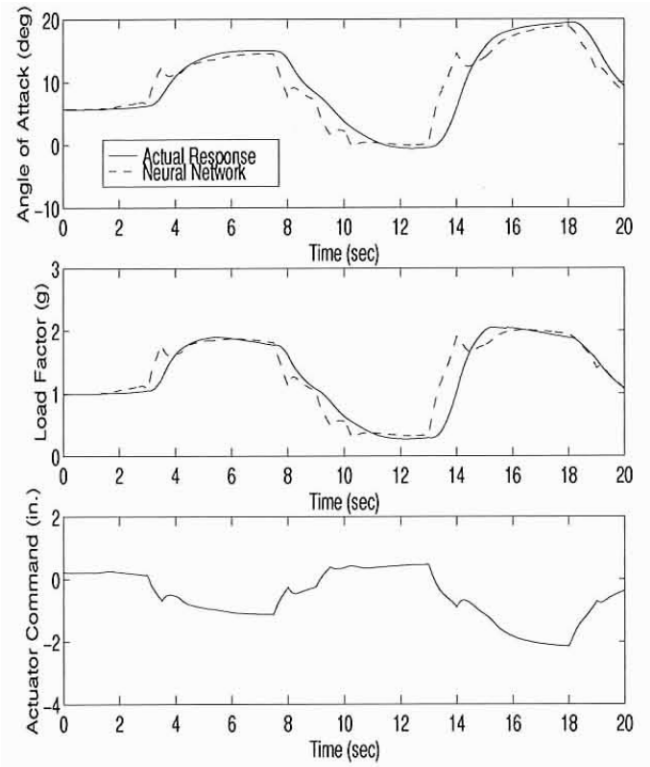

Figure 1.2.13 Neural Network performance [14]

1.3.The Focus of This Research and Contributions

This study focuses on keeping the main rotor speed inside limits during autorotative flight. During autorotation, the main rotor speed has maximum and minimum boundaries that should be avoided to prevent any risks of the helicopter crash, and/or any damage to the aircraft. All of the rpm limit exceedances do not result in fatal accidents, but they cause damages that require highly expensive maintenance or that are unrecoverable. Also, it is crucial to keep the rotor speed around nominal values in order not to lose the control authority. In 2015, a Robinson 22 helicopter crashed during pilot training. According to the crash report of AAIB[5], the instructor demonstrated an autorotation exercise and his student was supposed to perform a similar maneuver. During the attempt the rotor rpm decreased below the low rpm limit and, although the student further lowered the collective, the rotor could not regenerate enough lift force. The airspeed was reduced, and the descent rate was increased. The instructor applied full power to recover from the situation and to preserve height and airspeed. However, attempts to gain speed failed. At landing, the instructor attempted a flare maneuver, the skids dug in the ground, the rotors struck the ground and the helicopter rolled on its side. The crew was not injured but the rotor system and the tail boom were substantially damaged. After some time, the helicopter was reported destroyed, the damage was beyond repair. The lack of experience of pilots may lead to dangerous situations like this incident. A rotor rpm limit protection system may have been useful to prevent this accident.

Since autorotative flight is extremely hard for the pilots, decreasing the pilot workload during autorotation is a huge step in the safety of flight. For this purpose, the rotor speed is chosen as the limit parameter. Helicopter pilots' comments on rotor rpm behavior were consulted for initial insights. Using developed helicopter models, the response of rotor rpm to change of states and control inputs are investigated. Then, the rotor speed is estimated using a neural network-based algorithm. A collective control margin and pitch angle margin are calculated in real-time during flight simulation using the estimation models. These margins are used to cue the pilot model during autorotative flight and rotor rpm limits are avoided.

In the literature, comprehensive flight envelope protection studies were done for non-emergency flights. The studies on limit avoidance during autorotation in the literature were done using linear models of rotor speed. Linear models are not accurate enough for a highly nonlinear parameter such as rotor rpm with high importance concerning flight safety. Besides, these studies do not provide a margin for the rotor speed, but they propose a control input sequence to stay at a nominal rpm value. The rotor speed limit margin estimation and limit avoidance during autorotative flight is the contribution of this thesis to the literature.

1.4.Structure of the Thesis

The thesis is presented as follows: Chapter II starts by presenting the methodologies for helicopter modeling. Following, the developed rotor speed estimation model is presented. The model is developed using a Neural Network based algorithm which is also explained. The chapter is finalized with the explanation of the developed limit protection methods; one based on pitch margin estimation and the other one based on collective input margin estimation. The proposed envelope protection strategies that were developed using the estimated margins are presented. In Chapter III, the effectiveness of the developed limit protection methods is demonstrated. The simulation results for several maneuvers using the envelope protection algorithms are presented. Finally, in Chapter IV the results are discussed.

2. METHODOLOGY

2.1. Helicopter Mathematical Model

The general structure of the helicopter model is represented in Figure 2.1.1. The helicopter model was developed using Matlab Simulink environment. Each component of the helicopter was modeled separately.

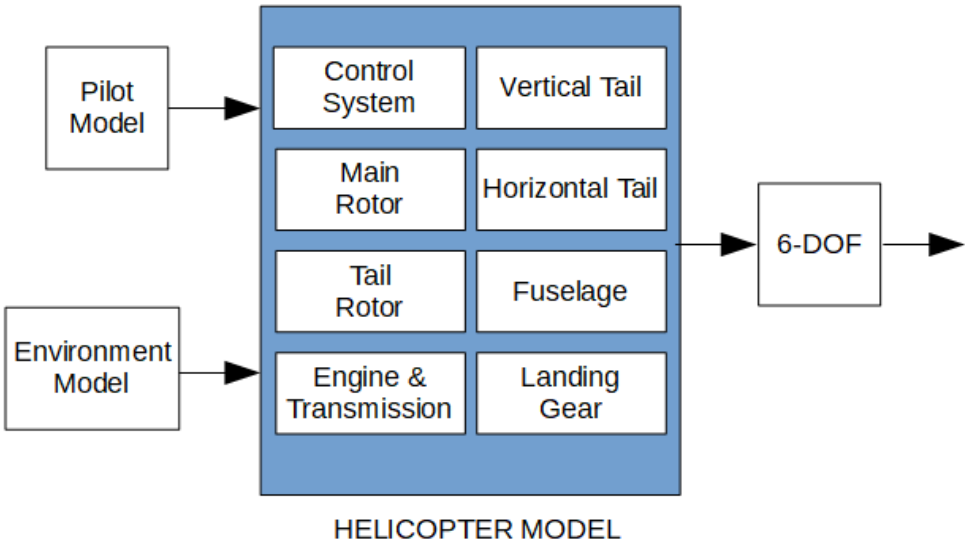

Figure 2.1.1 General structure of the helicopter model

The models are developed using physics-based functions. The environment model used in this study is a simple standard atmosphere model. The developed control system [15] gets the inputs from the pilot and calculates the corresponding blade angles of the main rotor and tail rotor. All resultant forces and moments calculated from each component are used in the calculation of 6-DOF equations of motion. The following chapters explain the modeling procedures in more detail.

2.1.1. Main Rotor

The main rotor dynamics and aerodynamics in the model consist of coupled dynamics of flapping and inflow dynamics. In the main rotor model, the Blade Element Theory and Pitt-Peters Dynamic Inflow Theory are used. These methods are proved in certified helicopter flight models that were developed in Aerotim Engineering LLC. and have proven high fidelity and reliability for helicopter flight simulation. The performance of these models at autorotative flight conditions is also proved to be realistic, hence the same methods are used in this thesis.

In this part of the chapter, the main rotor modeling method is explained. First, some general explanations are given for a better understanding of the main rotor system. Then, the basic inflow calculations and models in the literature are explained. Finally, the improved high fidelity dynamic inflow model is explained briefly.

The main rotor is the most important element of a helicopter. It has two important roles in flight; creating a lift force that will carry the weight, and creating a propulsive force for the horizontal motion. These forces are the projections on vertical and horizontal axes of the total thrust force that is perpendicular to the rotor disk.

In Figure 2.1.2, the blue rectangular represents the rotor disk plane and it is tilted with an angle,α towards the oncoming air velocity, V. The generated thrust providing both the lift force and the propulsive force is represented in this figure.

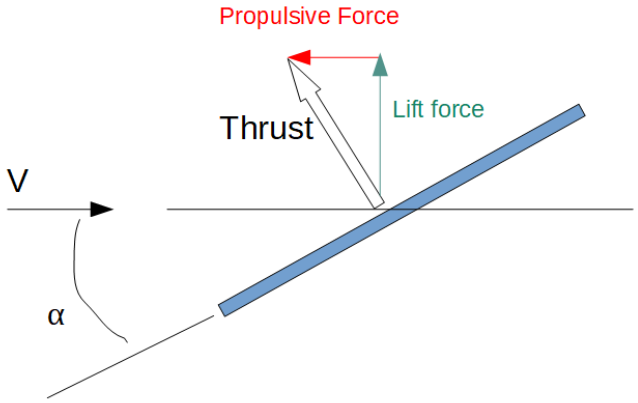

Figure 2.1.2 Rotor disk and thrust force orientation

V: Oncoming air velocity

α: Tip path plane angle

Conventional helicopters have two or more bladed rotor systems. These blades are attached to a central hub and are equally spaced. The rotating motion of the blades around the hub generates lift and drag forces on each blade. These forces produce the torque, thrust, and other forces and moments that are generated on the rotor. The large moments on the rotor and the high stresses on the blade are transmitted through the hub to the helicopter. To avoid these large moments, hinges are placed at the blade roots. These hinges allow a free motion to the blade which is normal to the disk plane and also in the disk plane [3].

Figure 2.1.3 shows an example hinge mechanism. This hinge mechanism enables to relieve the bending moments that are created on the blade and are transmitted to the hub. Some rotor hub designs eliminate the hinges and use structural bending rotor blades. The root forces and moments are higher but the main concept is kept, the blades are flexible to move in normal to and in disk plane directions.

The motion around the hinge that is placed horizontally to the disk plane is called the flapping motion. The motion around the vertically placed hinge is called lead-lag motion.

The general terminology of the rotor is explained in Figure 2.1.4. The azimuth angle is measured in the direction of rotation of the blade. 'r' is equal to zero at the center of rotation, and it is equal to R at the blade tip. For constant rotational speed,

$$\psi_b = \Omega t \tag{2.1.1}$$

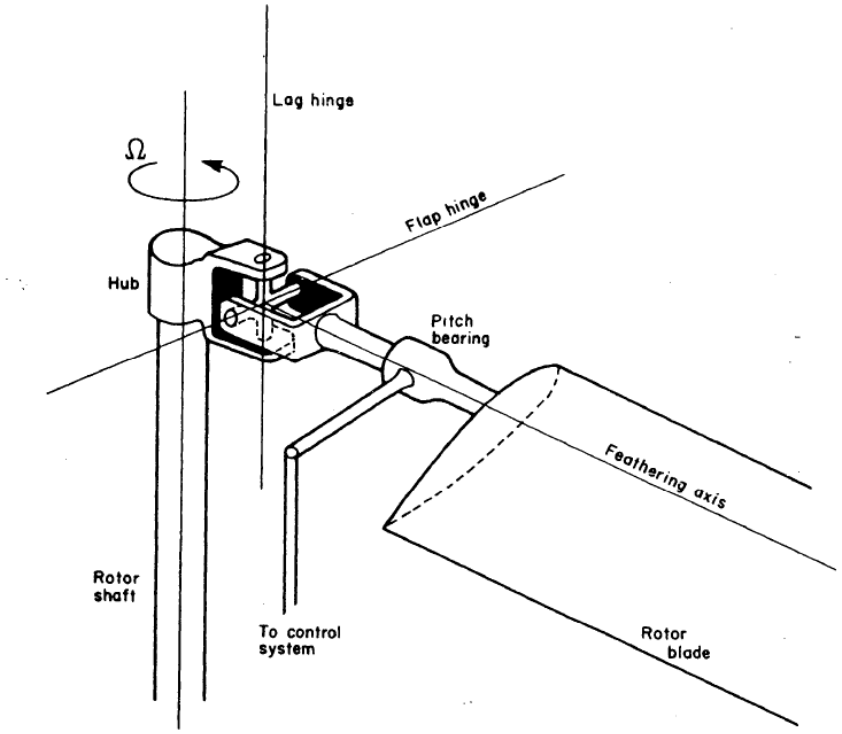

Figure 2.1.3 Schematic of an articulated rotor hub, showing only one blade structure [3]

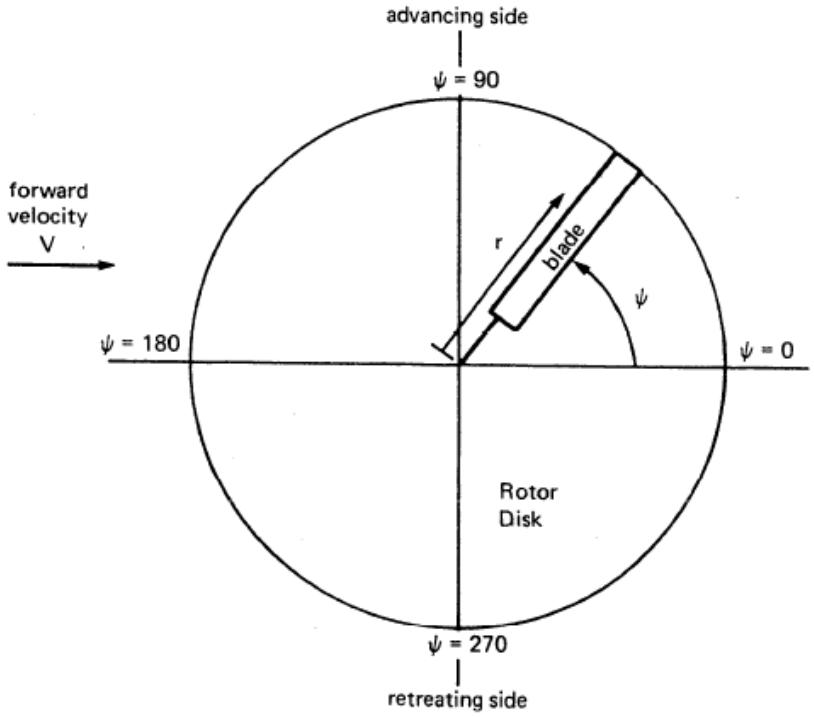

Figure 2.1.4 Rotor disk representation [3]

ψ_b: Azimuth of the blade, equals zero when the blade is at the downstream position.

r_b: The radial location of the blade which is measured from the center of rotation towards the blade tip.

R: Rotor radius measured from the hub to the blade tip

Ω: Rotational speed of the rotor

The blade motion is represented in Figure 2.1.5 in a simple form. Basically, the motion of the blade is a rigid body rotation about the rotor hub. The rotations of the blade about the hinges at the root are marked as $\beta_b, \zeta_b, \theta_b$ which are blade flap angle, blade lag angle, and blade pitch angle, respectively.

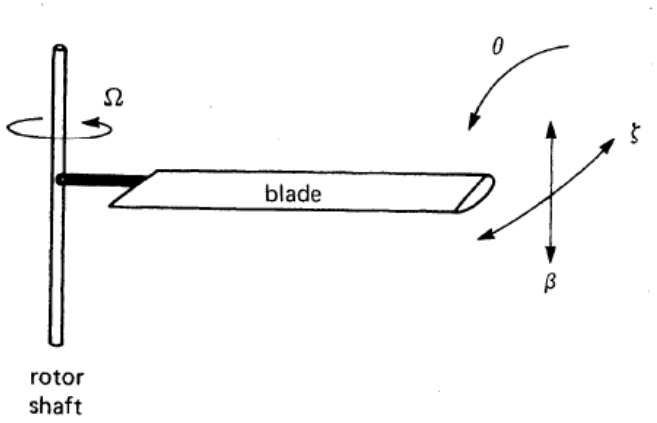

Figure 2.1.5 Fundamental blade motion [3]

The blade motion is defined as Fourier series which is periodic around the azimuth[3]:

$$\beta_b = \beta_0 + \beta_{1c}cos\psi + \beta_{1s}sin\psi + \beta_{2c}cos2\psi + \beta_{2s}sin2\psi + \cdots \quad (2.1.2)$$

$$\zeta_b = \zeta_0 + \zeta_{1c}cos\psi + \zeta_{1s}sin\psi + \zeta_{2c}cos2\psi + \zeta_{2s}sin2\psi + \cdots \quad (2.1.3)$$

$$\theta_b = \theta_0 + \theta_{1c}cos\psi + \theta_{1s}sin\psi + \theta_{2c}cos2\psi + \theta_{2s}sin2\psi + \cdots \quad (2.1.4)$$

β_0: Rotor coning angle

β_{1c} : Pitch angle of the tip-path plane

β_{1s}: Roll angle of the tip-path plane

θ_0: Rotor collective pitch

θ_{1c}, θ_{1s}: Cyclic pitch angles

The 0, 1c, and 1s Fourier coefficients which are the mean and first harmonics of the blade motion are the most important harmonics for the rotor performance and control. Higher harmonics ($\beta_{2c}, \zeta_{2c}, \theta_{2s}$ ... etc) are neglected in calculations for simplicity.

The Minimum Complexity Method [16] is used in literature to develop a simple mathematical model for the rotor and other helicopter components. This is a simulation

helicopter math model developed by NASA in 1988 and is still being used for real-time helicopter simulations. The model was developed with an intention of decreasing computational delays, cost, and inflexibility of the very sophisticated math models. In this thesis, the component models other than the main rotor are based on the Minimum Complexity model. Each component is explained in the following parts of this chapter.

The relationship between thrust, power, and airspeed is particularly important while modeling the main rotor. This relationship defines the induced velocity of air passing through the rotor disk. In the minimum complexity model, the induced velocity effects are modeled with the classical momentum theory, where the thrust and induced-velocity are solved through an aerodynamic feedback loop. The computation is complicated due to the high non-linearity of the feedback. The induced velocity and vertical thrust force are calculated using the simple momentum equation by iterating the inflow for a few timesteps. In a real-time simulation, this iteration should be improved. Hence, the dynamic inflow models were developed in the literature and the fidelity of the main rotor models was highly improved[4].

The basic thrust equation by the Glauert momentum model is [17]:

$$T = 2\rho A V' w_w \tag{2.1.5}$$

where

$$V' = \sqrt{((u_0 + w_w cos\beta_m)^2 + (w_0 - w_w sin\beta_m)^2)} \tag{2.1.6}$$

T: Thrust

V': The net air velocity

w_w: Inflow (induced velocity)

β_m: Mast angle

u_0, w_0: Air velocities on the rotor disk

Figure 2.1.6 shows the representation of the rotor disk and the oncoming air velocity vectors.

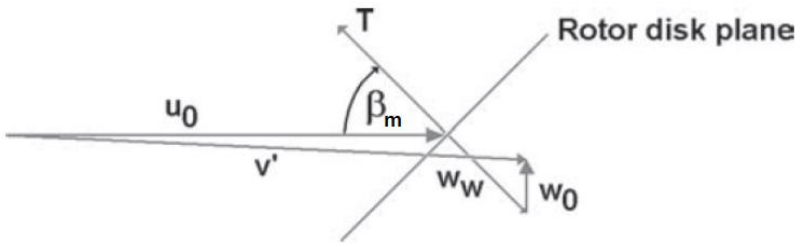

Figure 2.1.6 Rotor disk plane with an arbitrary mast angle β_m [4]

The momentum theory estimates the rotor performance using the basic conservation laws of fluid mechanics. The action of the air on the blades creates a thrust in the rotor disk. As a result of the opposite reaction of the rotor on the air by Newton's law, the velocity of air in the rotor wake increases in the opposite direction to the thrust. The rotor is modeled as an actuator disk which is an approximation to the actual rotor. It is a circular surface with zero thickness that accelerates the air through the disk by creating a pressure difference. According to the Glauert momentum model, the thrust is actually the momentum flux. Where w_w is the induced velocity and V' is the net velocity of oncoming air on the rotor disk.

Using non-dimensionalized velocities, the thrust equation (2.1.5) results in the momentum theory fourth-order polynomial representing induced velocity in vertical and horizontal flight at arbitrary incidence to the oncoming wind. u_0 and w_0 are the airspeeds on rotor hub x and z-axis directions.

The induced velocity at hover is given as:

$$w_{w_0} = \sqrt{\frac{T}{2\rho\pi R^2}} \tag{2.1.7}$$

w_{w_0}: Inflow (induced velocity) at hover condition

T: Thrust

ρ: Air density

R: Rotor radius

Using the hover induced velocity, the non-dimensionalized velocities are defined as:

$$\acute{w} = \frac{w_w}{w_{w_0}}, \acute{\mu} = \frac{u_0}{w_{w_0}}, \acute{\eta} = \frac{w_0}{w_{w_0}} \tag{2.1.8}$$

$\acute{w}$: Non-dimensional induced velocity

$\acute{\mu}$, $\acute{\eta}$: Non-dimensional horizontal and vertical airspeeds

Implementing these relations into the thrust equation (2.1.5) gives:

$$\acute{w}^4 + 2\acute{w}^3(\acute{\mu}cos\beta_b - \acute{\eta}sin\beta_b) + \acute{w}^2(\acute{\mu}^2 + \acute{\eta}^2) - 1 = 0 \tag{2.1.9}$$

This is the momentum theory fourth-order polynomial representing the induced velocity in vertical and horizontal flight at arbitrary incidence to the oncoming wind.

Some iterative procedures are required to find the solution to this polynomial. The dynamic modeling method suggested by [4] is used to solve this in the model instead of the one used in the minimum complexity method to improve real-time responses of the main rotor. This method assumes that the rotor is placed at the center of a sphere, which has a radius on some divided element of the rotor blade. The air mass inside the sphere is accelerated by the motion of the rotor and generated thrust, the equation of Glauert's momentum theory can be rewritten as:

$$T = 2\rho AV' w_w + \frac{4}{3}\pi(kR)^3\rho\dot{w}_w \tag{2.1.10}$$

The second part of the equation is also called the effect of the apparent mass. For known thrust T and inflow w_w at a given simulation time, $\dot{w}_w$ is solved as:

$$\dot{w}_w = \frac{T - 2\rho A V' w_w}{\frac{4}{3}\pi(kR)^3\rho} \tag{2.1.11}$$

The value of k can be selected between 0.74 and 0.86 as suggested in [4] for the convergence of the inflow iteration in time. According to the Pitt-Peters inflow model, k is selected to be 0.8 for convergence. To further improve the inflow model, some corrections and improvements on the inflow model are done as suggested in Pitt-Peters dynamic inflow model [18]. This high fidelity inflow model was developed in Aerotim LLC, and the same methods are used in the UH-60 helicopter model that is used in this thesis. The developed model in Aerotim LLC. is proved to be reliable and it is certified by authorities. Hence, it is convenient to use in this study for investigating the autorotation dynamics and developing a flight envelope protection system.

2.1.2. Main Rotor and Engine Drive Train

The transmission is modeled by using the model suggested by Dreier [4]. In a helicopter, the engine powers the rotor, generator, air conditioner, and other equipment. The power distribution is done by the drive train. Drive train includes transmissions, gearboxes, drive shafts end clutches, etc. The engine power is transferred in a transmission to the drive shaft, which distributes the power to the rotor and accessories. In autorotation, the main rotor also provides power to keep the tail rotor turning, as well as providing enough thrust to glide the helicopter.

In autorotation and an event of engine failure, the clutch mechanism enables the rotor to drive the tail rotor. The schematic of the system is shown in Figure 2.1.7.

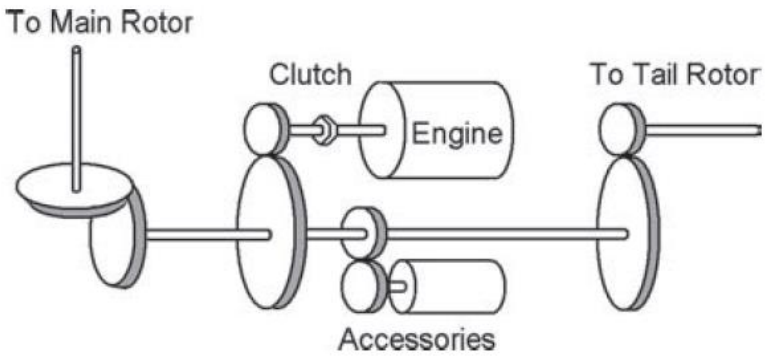

Figure 2.1.7 Main Rotor and Engine Drive Train[4]

Figure 2.1.8 shows the engine drive train as an information flow diagram in a schematic that could be modeled using the Matlab Simulink tool. In [4], this representation is written for a double engine – single rotor helicopter. The drive train for Engine 1 is shown in this figure since the second engine also has the same dynamics and representation. The subscript 1 in the figure represents Engine 1. UH-60 is a single-engine single rotor helicopter, hence the model also consists of a single-engine.

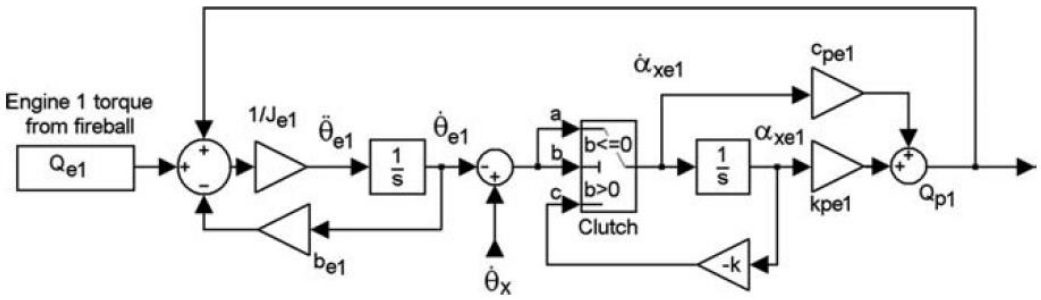

Figure 2.1.8 Schematic representation of the equation of drive train[4]

The difference represented with $\dot{\alpha}_{xe1}$ is the difference between $\dot{\theta}_x$, which is the transmission speed from the rotor, and $\dot{\theta}_{e1}$, the engine speed. $\dot{\alpha}_{xe1} = \dot{\theta}_x - \dot{\theta}_{e1}$. As seen from Figure 2.1.10, the clutch mechanism uses the continuous variable $\dot{\alpha}_{xe1}$ as the switch logic.

The general dynamic model of a drive train element[4] can be written by the equations:

$$J_e\ddot{\theta}_e = Q_e + Q_p - b_e\dot{\theta}_e \tag{2.1.12}$$

$$Q_p = c_{pe}\left(\dot{\theta}_x - \dot{\theta}_e\right) + k_{pe}(\theta_x - \theta_e) \tag{2.1.13}$$

J_e: Engine inertia

$\dot{\theta}_e$: Engine speed

Q_e: Engine torque

$\dot{\theta}_x$: External transmission speed

Q_p: Shaft torque of the power turbine

'c' and 'k' represent the damping and stiffness of the shaft respectively. The engine is assumed to have a mass and its polar inertia is J_e. It is also assumed to have a case drag, which is calculated as $b_e\dot{\theta}_e$. An internal torque Q_e, is assumed to be generated when the engine shaft experiences a dynamic deformation. The values of the damping and stiffness coefficients are selected as suggested in [4], and the model response is improved after changing the coefficients by trial and error.

The clutch switch is the important section of this model. The difference between the rotor speed and engine speed determines whether the engine is clutched or not. If the difference is less than zero, this means the engine drives the rotor, the clutch is used as a rigid link. If the difference is greater than zero, the engine is declutched. This means the engine is slower than the main rotor and freewheeling is required.

2.1.3. Other Components of the Helicopter Model

The tail rotor model uses the same method for the calculation of forces and induced velocity generated in the tail rotor, but the flapping effects are not included in the calculations.

The fuselage model generates forces due to drag, and the drag is calculated by assuming an equivalent flat plate drag area for each axis. These forces are also used to calculate the generated power and contributes to the calculation of the torque.

The forces are calculated at the center of pressure of the fuselage. Then they are transformed to the center of gravity of the helicopter. The force equations are in a quadratic aerodynamic form [16] which is the drag in any direction of flight limiting the speed. The equivalent flat plate areas for each axis and the center of pressure are calculated using the geometric values of the UH-60 helicopter [15] [19].

The relation to calculate the resultant forces acting on the fuselage:

$$F_{FUS_{x,y,z}} = 0.5 * \rho * A_{FUS_{x,y,z}} * {V_{FUS_{x,y,z}}}^2 \quad (2.1.\ 14)$$

$A_{FUS_{x,y,z}}$: The equivalent flat plate drag areas on each axis of fuselage local body axes

$V_{FUS_{x,y,z}}$: Air velocity on fuselage local body axes

The moments can be calculated as:

$$M_{FUS_x} = F_{FUS_y} * R_{\mathrm{FUS_z}} + F_{FUS_z} * R_{\mathrm{FUS_y}} \quad (2.1.\ 15)$$

$$M_{FUS_y} = F_{FUS_z} * R_{\mathrm{FUS_x}} - F_{FUS_x} * R_{\mathrm{FUS_z}} \quad (2.1.\ 16)$$

$$M_{FUS_z} = -F_{FUS_x} * R_{\mathrm{FUS_y}} \quad (2.1.\ 17)$$

$R_{\mathrm{FUS_{x,y,z}}}$: Position vector between fuselage center of pressure and helicopter center of gravity.

The center of pressure of the fuselage, the helicopter center of gravity and R_{FUS} is represented in Figure 2.1.9. Fuselage local body axes are shown in Figure 2.1.10.

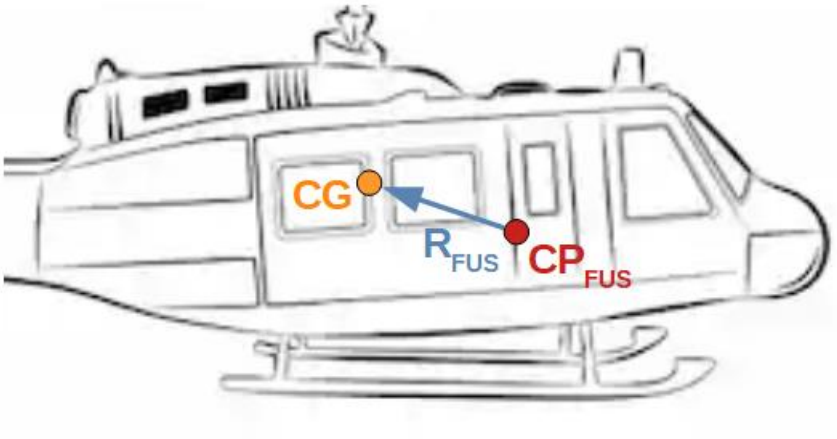

Figure 2.1.9 Fuselage center of pressure and position vector

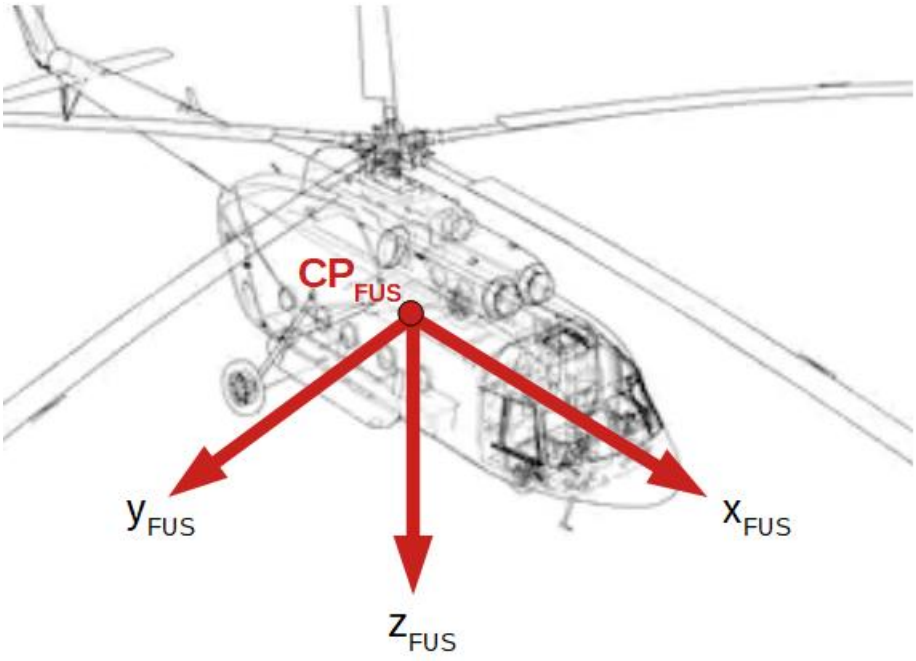

Figure 2.1.10 Fuselage local body axes, centered at the center of pressure of the fuselage

The horizontal tail model consists of a lift generated by an airfoil. The horizontal tail model is also based on the minimum complexity model. The horizontal tail is assumed to

generate force only in the z-axis. The forces on the y and x axes are neglected. Horizontal tail local body axes and position vector are shown in Figure 2.1.11.

The important part of modeling the horizontal tail is to compute the rotor downwash effect on the horizontal tail that affects the wind velocity around the horizontal tail, which affects the generated forces.[16]

The vertical force and moment generated by the horizontal tail is

$$F_{HT_z} = 0.5\rho\left(A_{xx_{HT}} V_{HT_x}^2 + A_{xz_{HT}} V_{HT_x} w_{HT}\right) \quad (2.1.\ 18)$$

$$M_{\mathrm{HT_y}} = F_{HT_z} * R_{\mathrm{HT_x}} \quad (2.1.\ 19)$$

$A_{xx_{HT}}$, $A_{xz_{HT}}$: The equivalent drag areas of the horizontal tail on horizontal and vertical sections.

w_{HT}: The net vertical velocity acting on the horizontal tail due to main rotor downwash

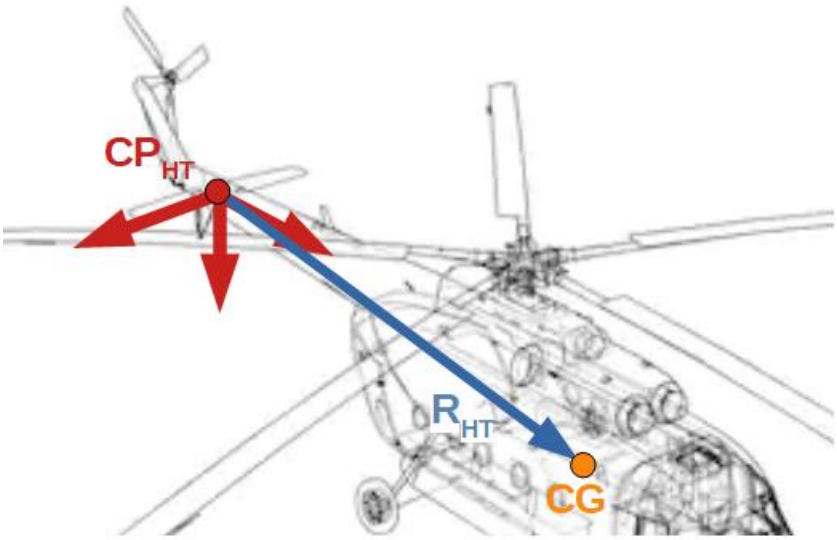

Figure 2.1.11 Horizontal tail local body axes system

The vertical tail is also calculated in the same manner as the horizontal tail, without the calculation of the main rotor downwash. The interaction between the rotor and the vertical tail, as well as fuselage and vertical tail, is neglected.

2.1.4. General Helicopter Dynamics

The equations of motion of the helicopter [20] are presented in this chapter. The forces and moments are defined at the center of gravity of the helicopter, on body-fixed axes.

The resultant force vector $\boldsymbol{F_{cg}}$ **:**

$$\boldsymbol{F_{cg}} = [X; Y; Z] \tag{2.1. 20}$$

X: The resultant force on helicopter x body axis

Y: The resultant force on helicopter y body axis

Z: The resultant force on helicopter z body axis

$$\dot{u} = -(wq - vr) + \frac{X}{m} - g\ sin\theta \tag{2.1. 21}$$

$$\dot{v} = -(ur - wp) + \frac{Y}{m} + g\ cos\theta\ sin\phi \tag{2.1. 22}$$

$$\dot{w} = -(vp - uq) + \frac{Z}{m} + g\ cos\theta\ cos\phi \tag{2.1. 23}$$

u, v, w : the linear velocities on helicopter body x,y, and z axis respectively.

p, q, r : the angular velocities on helicopter body x,y, and z axis respectively.

m: aircraft mass

ϕ, θ, ψ: the Euler rotations defining the orientation of the helicopter

The resultant moment at the center of gravity $\boldsymbol{M}_{cg}$

$$\boldsymbol{M_{cg}} = [L; M; N] \tag{2.1. 24}$$

L: The resultant moment on helicopter x body axis

M: The resultant moment on helicopter y body axis

N: The resultant moment on helicopter z body axis

$$\dot{p} = \frac{1}{(I_{xz}^2 - I_{xx}I_{zz})}\big(qr\big(I_{zz}^2 - I_{zz}I_{yy} + I_{xz}^2\big) - qpI_{xz}\big(I_{zz} - I_{yy} + I_{xx}\big) - (I_{zz}L + I_{xz}N)\big) \tag{2.1. 25}$$

$$\dot{q} = \frac{1}{I_{yy}}(M + pr(I_{zz} - I_{xx}) - (p^2 - r^2)I_{xz}) \tag{2.1. 26}$$

$$\dot{r} = \frac{1}{(I_{xz}^2 - I_{xx}I_{zz})}\Big(qrI_{xz}\big(I_{zz} - I_{yy} + I_{xx}\big) - qp\big(I_{xz}^2 - I_{yy}I_{xx} + I_{xx}^2\big) - (I_{xz}L + I_{xx}N)\Big) \tag{2.1. 27}$$

The resultant forces and moments are the summations of all forces and moments calculated at each helicopter component.

2.2.Rotor Speed Estimation Model

2.2.1. Investigation of the Rotor Speed Behaviour in Autorotation

As discussed in Chapter 1, the rotor speed limits are selected as the main concern for this thesis. An investigation of several parameters and their effects on the rotor speed showed that the collective input and pitch angle change is steady-state critical in rotor speed response. The study is based on the assumption that the rotor speed responds as a fast state for a given collective input or a pitch angle reference.

The investigation of the rotor speed response to the given inputs or change in parameters is performed by developing a pilot model. The pilot model is a PID controller that works

on four channels consisting of longitudinal, lateral, directional, and vertical controllers. The total control inputs acting on the helicopter model are saturated with real limitations of the control system so that the inputs are not unrealistic.

The derivatives in PID controllers are the stabilization in longitudinal, lateral, and directional channels. They are trying to keep the angular velocities of the helicopter at zero value using longitudinal and lateral cyclic, and pedal inputs. The longitudinal controller gets a pitch angle reference and generates a longitudinal cyclic input. The lateral controller gets a roll angle reference, which is the constant roll angle at the trim point, and it generates a lateral cyclic input. The directional controller gets a heading reference, which is also set to the trim heading value. It generates a pedal input. The vertical controller gets a vertical speed reference and generates corresponding collective input.

As mentioned in Chapter 1, the helicopter pilots use the pitch attitude and the collective input to control the rotor speed during autorotation. The first thing that comes to mind is that the longitudinal cyclic input is being used to control the rotor speed. To investigate this behavior, a longitudinal cyclic step input is given to the helicopter model at different autorotation trim points. It is concluded that the longitudinal cyclic can not be used to estimate the rotor speed, because after a cyclic step input the helicopter does not converge to a trim state. The pitch angle continues to change and it diverges until the longitudinal cyclic input is reversed.

Due to the divergent behavior of the helicopter after a longitudinal cyclic step input, it was decided to investigate the behavior after a step input change in the pitch angle reference. The main rotor speed is investigated after a given step input in pitch angle reference to the helicopter model trimmed in autorotation. The pilot model tracked the given pitch angle reference. The collective is held constant at the trim point, while roll and heading angles are kept in the trim state with lateral cyclic and pedal inputs. The rotor speed converged to a steady-state value as the pitch angle reaches its new steady-state value. Some examples of the behavior are presented below. It should be noted that the

responses that are presented include both the helicopter dynamics and the controller dynamics of the pilot model.

A step pitch reference is given to the pilot model at different trim conditions. Several examples of the rotor speed response to pitch up and down reference inputs at different trim points are shown in Figures 2.2.1 to 2.2.4. Figure 2.2.1. shows a pitch up reference and corresponding rotor speed response at 65 knots forward speed autorotation.

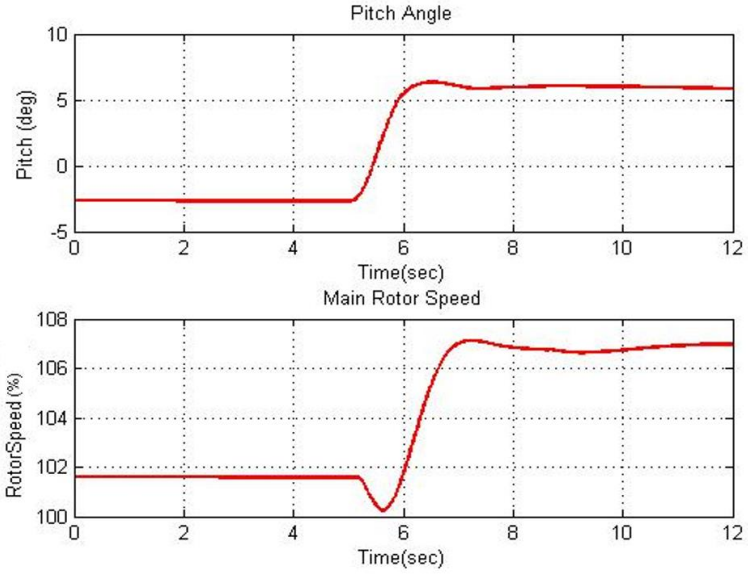

Figure 2.2.1 Pitch up reference at 65 knots forward speed autorotation

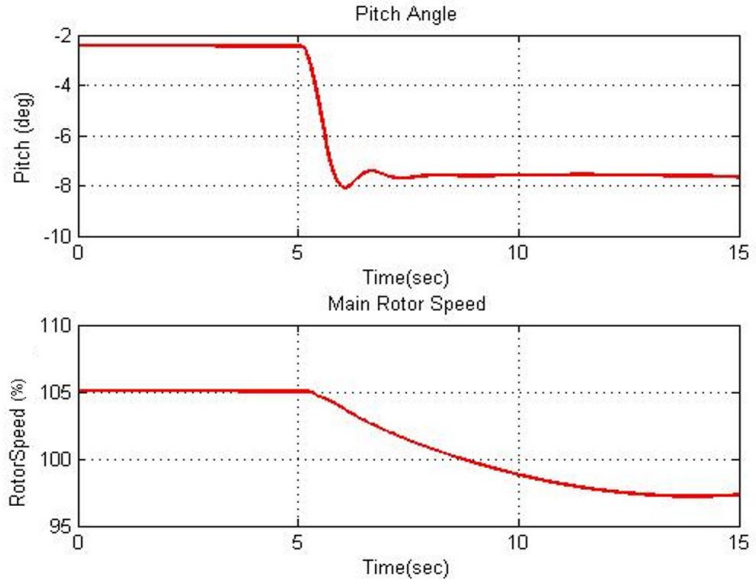

Figure 2.2.2 Pitch down reference at 65 knots forward speed autorotation

The rotor speed increases as the pitch angle increases and it converges to a trim value. After a few seconds, the rotor rpm changes since the collective is fixed, the airspeed decreases at this nose-up position. Hence, only a few seconds of rotor speed is shown in the figures.

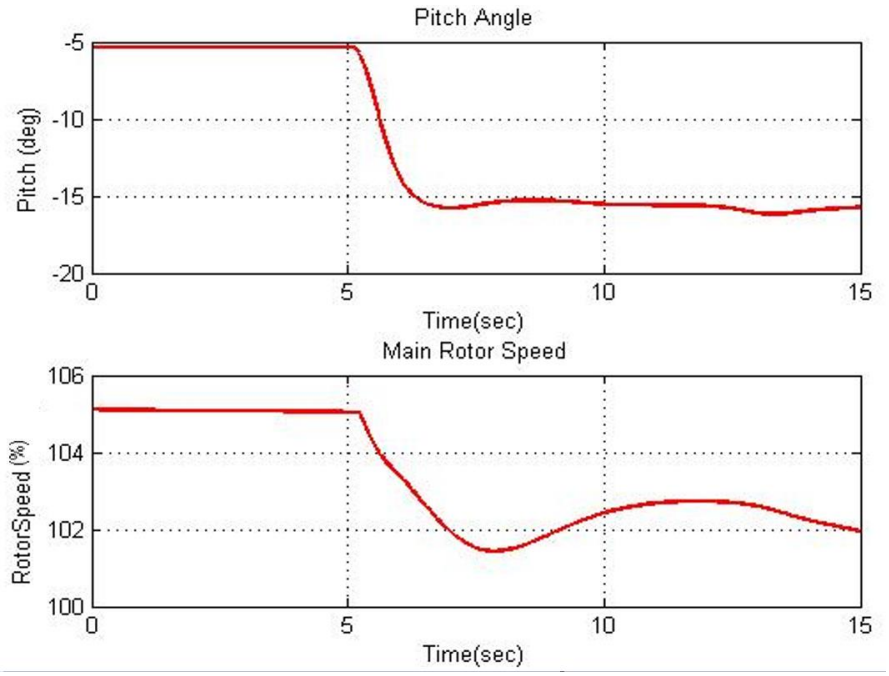

Figure 2.2.3 Pitch down reference input at 90 knots forward autorotation

When the helicopter pitch angle increases to a nose-up position, the total amount of airflow through the rotor disk increases, but after some time since the airspeed decreases, the airflow also decreases. Similarly, in a nose-down situation, the airflow through the rotor disk decreases.

Figure 2.2.2 shows a trim point also at 65 knots but with a higher vertical speed, pitch down reference is given to the pilot model. Figures 2.2.3 and 2.2.4 show trim points at 90 knots forward autorotation, pitch up and pitch down references were given to the pilot model and the rotor speed response is shown. From the results, it can be stated that the rotor speed is steady-state critical to a pitch angle change.

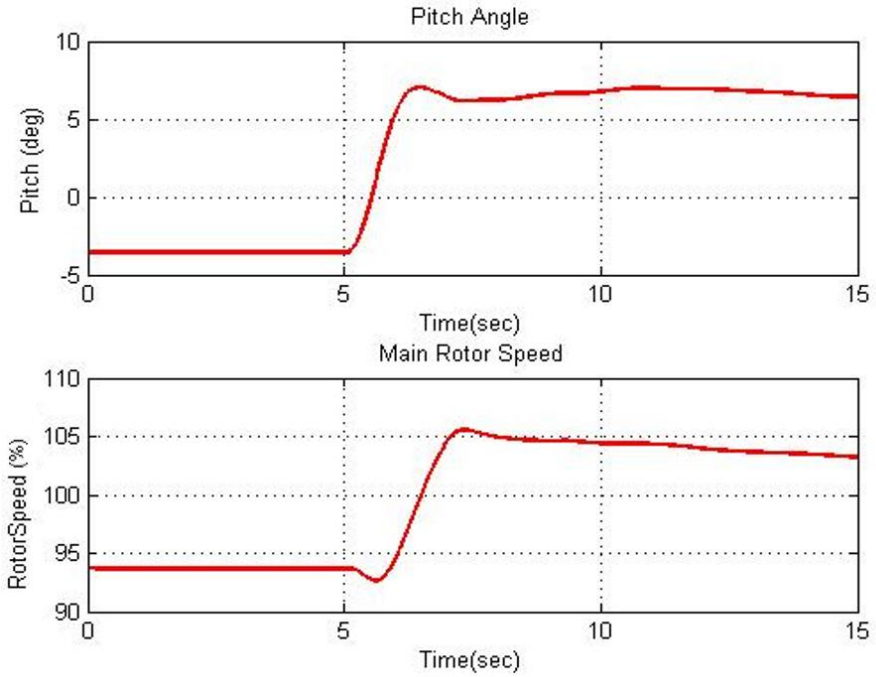

Figure 2.2.4 Pitch up reference input to 90 knots forward autorotation

The same procedure is performed for the collective input. The following figures (Figure 2.2.5 to Figure 2.2.8) show some example rotor speed responses to given step collective inputs.

As can be seen from the rotor speed responses, it can be stated that the rotor speed is steady-state critical to a given collective input.

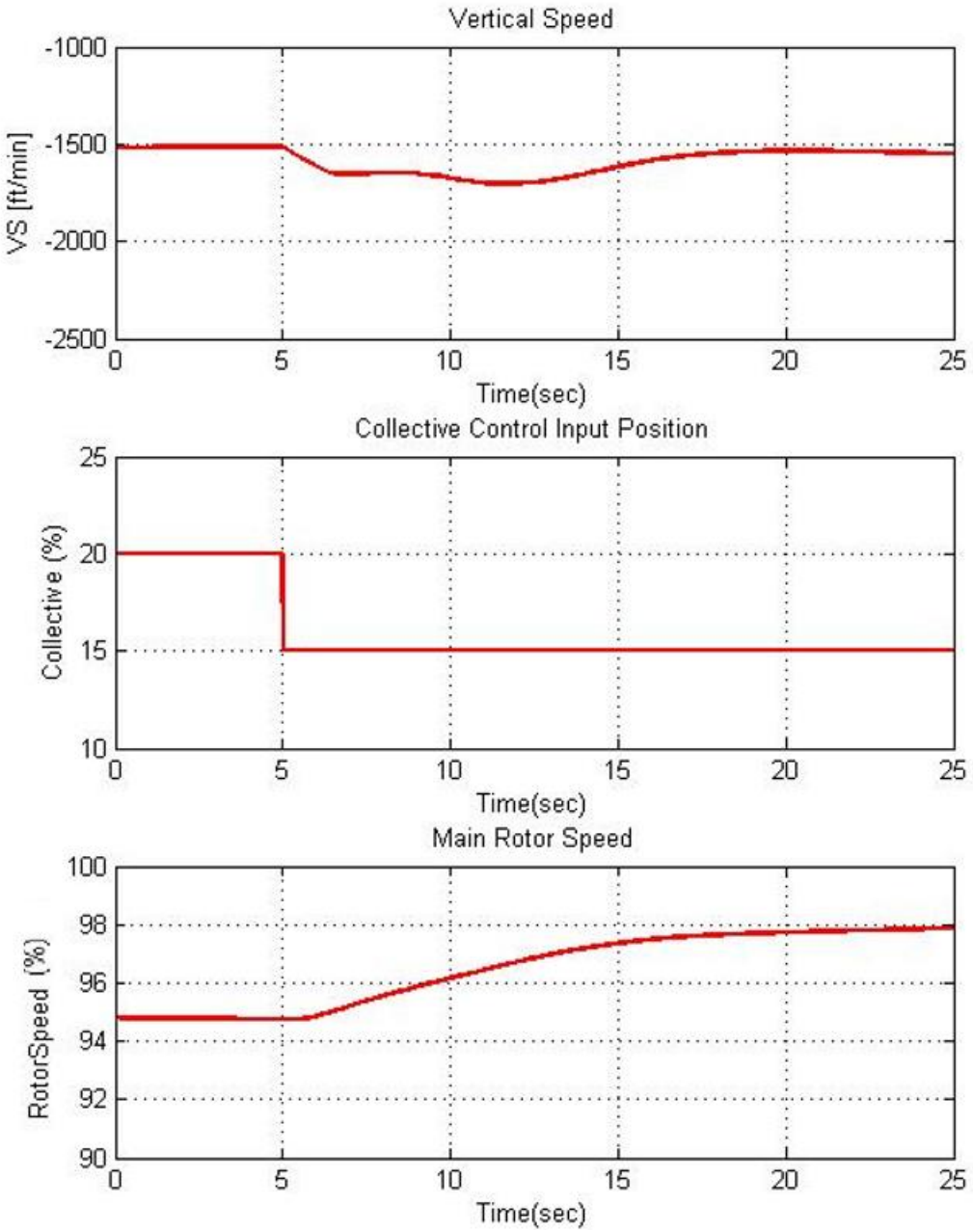

Figure 2.2.5 Collective step down input at 65 knots autorotation

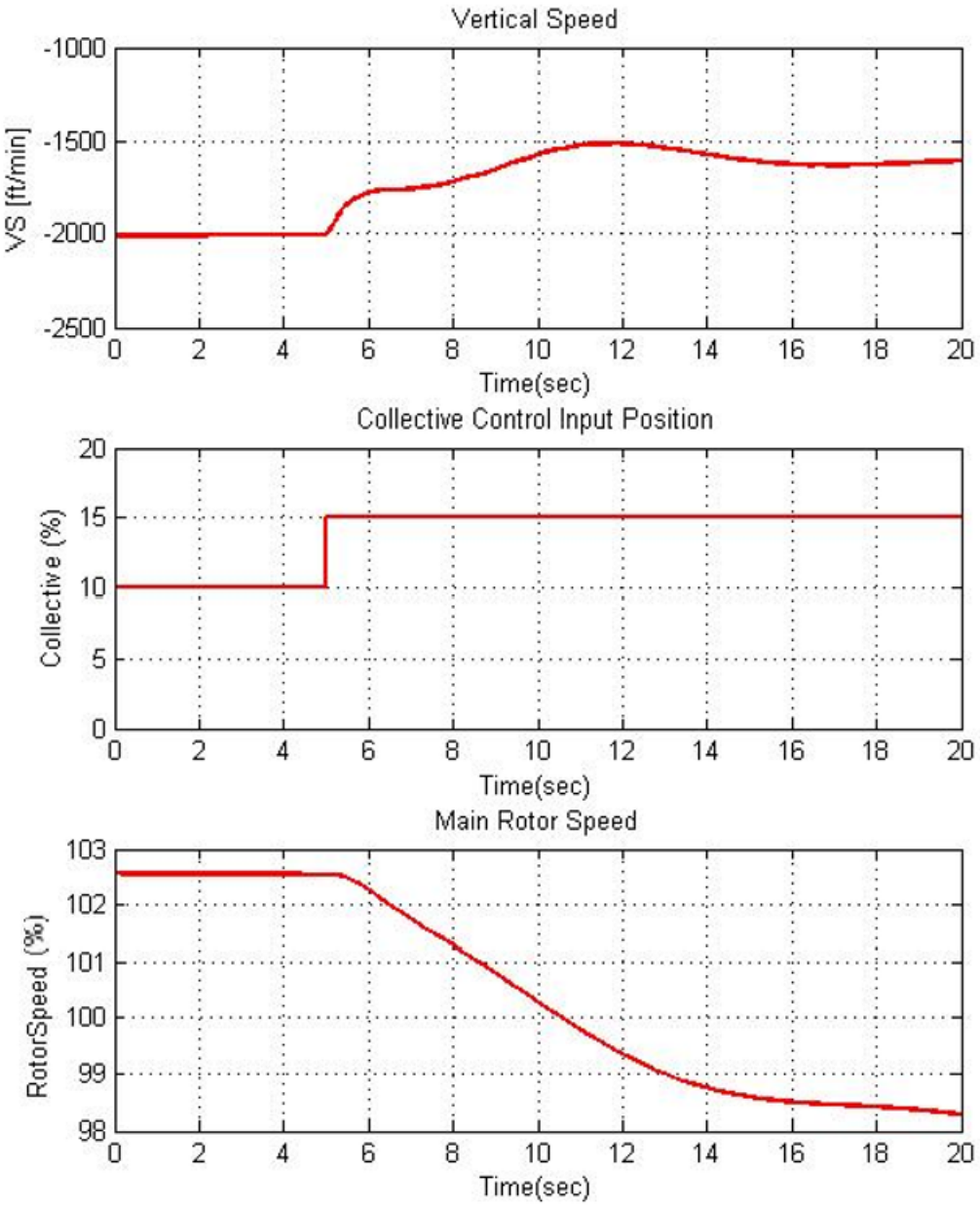

Figure 2.2.6 Collective step-up input at 65 knots autorotation

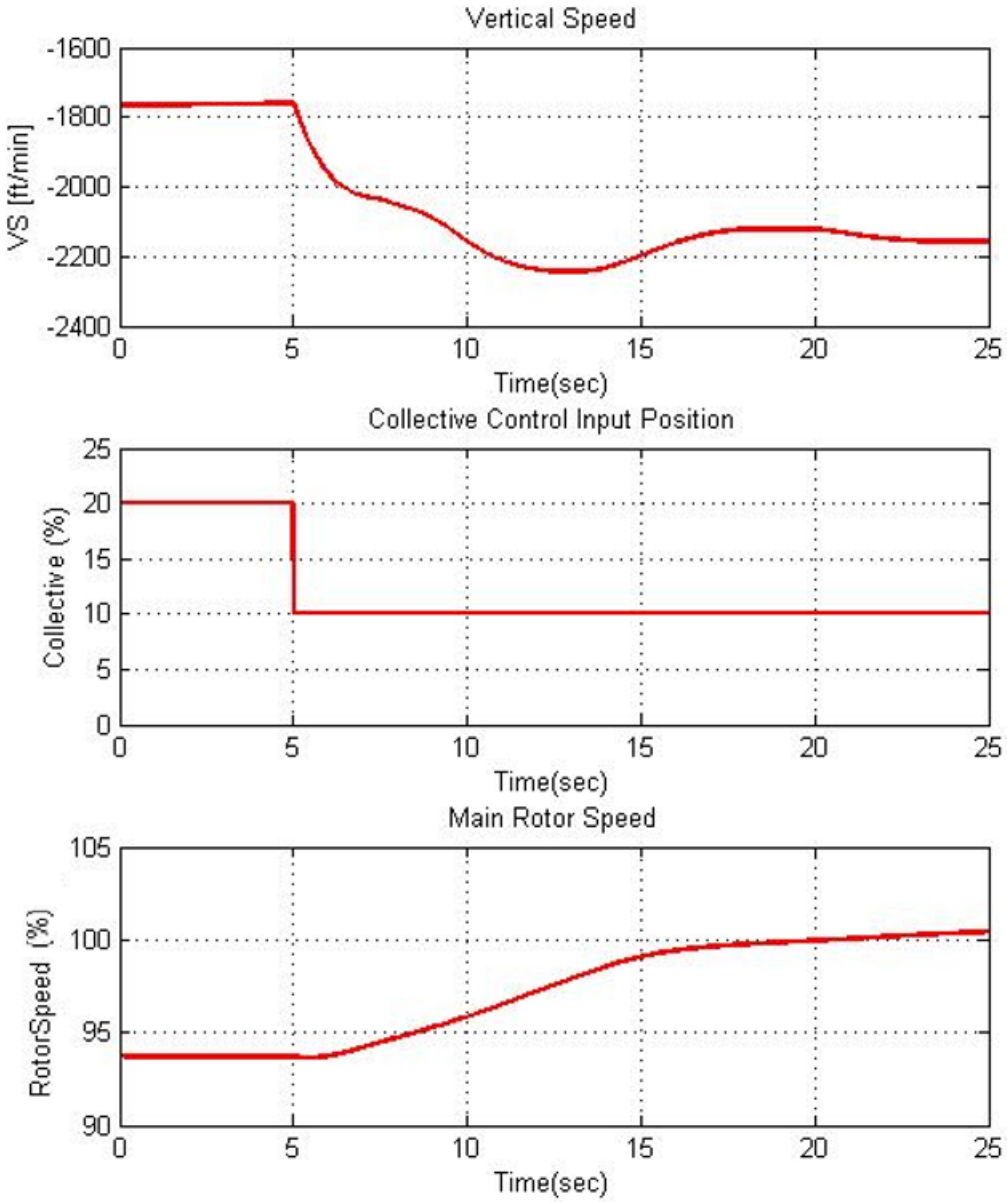

Figure 2.2.7 Collective step down input at 90 knots autorotation

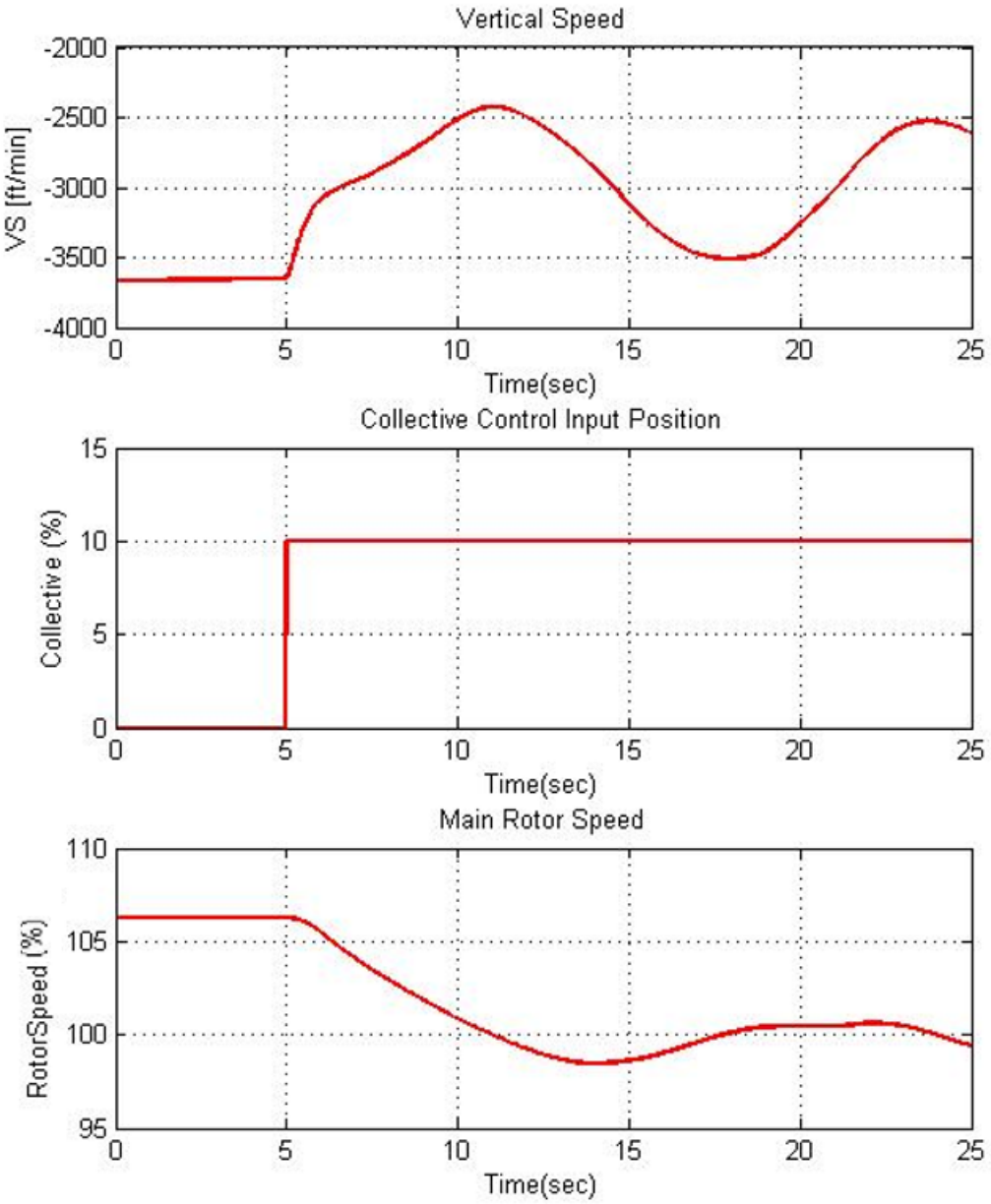

Figure 2.2.8 Collective step-up input at 95 knots autorotation

After it was decided that the rotor speed is a fast state for a given collective input and a pitch angle reference, the rotor speed estimation model was developed. The estimation model is a function of collective input, pitch angle, and the rotor hub velocities.

The aircraft states can be grouped as ‘fast’ and ‘slow’ states. Dynamic trim is a maneuvering steady-state condition, meaning the trimming of the fast aircraft states. The slow states may be changing during dynamic trim. The fast states, for example, angular

rates, load factor, angle of attack, converges to equilibrium quickly after a control input is given to the aircraft. Whereas the slow states converge slowly, for example, airspeed. Since the fast states reach the equilibrium faster, they can be used for the estimation of future slow states[13].

A dynamic trim database for autorotation flight is generated and a neural network model is created and trained offline using this trim database. The trim database is selected such that it includes as many flight conditions as possible that might be encountered during autorotative flight[21]. This model is used for online RPM estimation during autorotative flight.

2.2.2. Neural Network Approximation for Rotor Speed

The rotor rpm is estimated by a function based on the pitch angle, pilot collective input, and the rotor hub velocities on the x, y, and z axes. This approach is a modified approach from [8] where local hub velocities and pilot collective and pedal inputs during flight were used to predict the main rotor torque during normal flight. In this thesis, the torque will be zero since the investigated flight condition is autorotation, and the parameter that should be monitored and controlled is the rotor rpm. Based on the previous investigation of the parameter, the rotor speed is estimated as:

$$\Omega_{pred} = f(\sigma_{coll}, \theta, V_{xhub}, V_{yhub}, V_{zhub}) \quad (2.2.1)$$

where Ω_{pred} is the predicted rotor speed, θ is the helicopter pitch angle, σ_{coll} is the collective input position, and $V_{xhub}, V_{yhub}, V_{zhub}$ are the rotor hub velocities on the x, y, and z axes of the local hub axis. A neural network algorithm is used to estimate this relation.

The general structure of a neural network is shown in Figure 2.2.9. Artificial neural networks were developed with a desire to imitate the brain, which is a biological system composed of neurons. A neural network can be defined as a system of processing

elements which are called neurons. The neurons are connected with each other into a network by a set of weights. The magnitude of weights, the architecture of the network structure, and the processing operation mode determines the final resultant function of the neural network [22]. The neuron is an element that processes the data. It may take several inputs. These inputs are multiplied with the associated weights in the neuron, to differentiate the importance of each input in the calculation. Then, the weighted inputs are summed up, and the result is a singular valued function which is called the activation function. The nodes are marked with the sum operator in Figure 2.2.9. 'W' indicates the weights. 'u' and 'x' are the control inputs and states of the system. The activation functions output the estimated limited parameter.

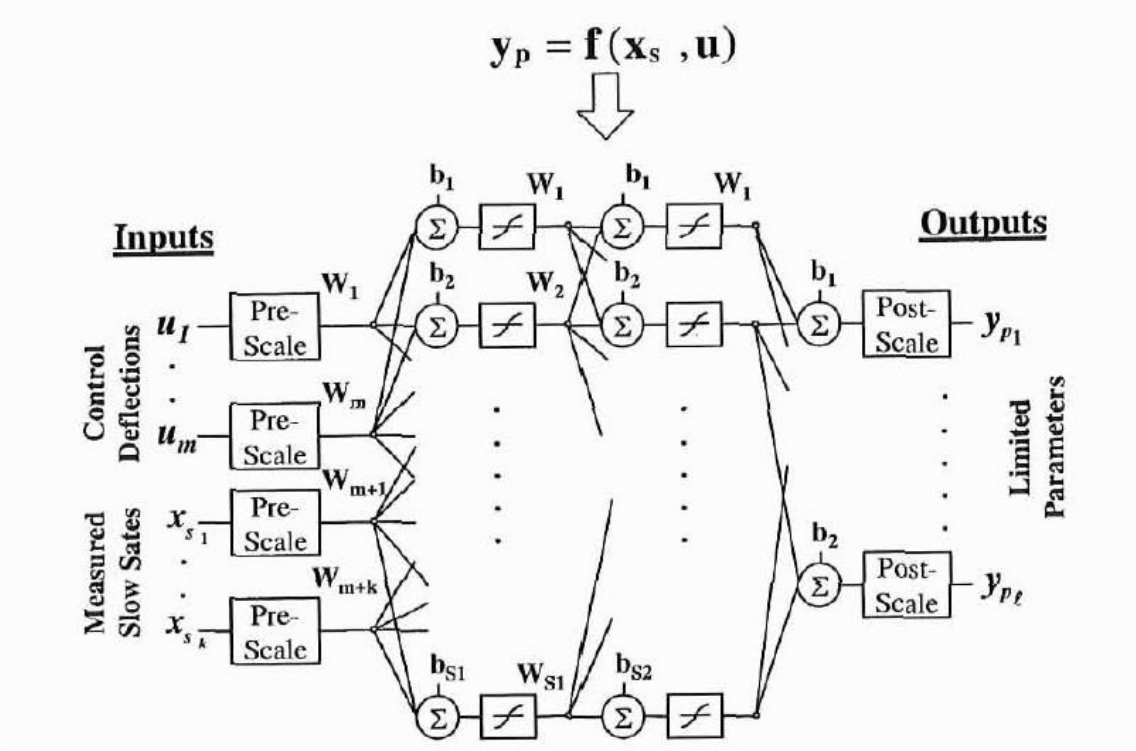

Figure 2.2.9 Neural Network Architecture[14]

The inputs to a neuron can be external inputs, like the control deflections or states, as well as outputs of other neurons. Adding neurons after neurons create a structure that is called multilayer neurons. The activation functions may take any form It can be a linear function,

a hyperbolic tangent, a sigmoid function, or a step function, but most often the function is monotonic[22].

Similar studies in the literature suggested that neural networks were efficient to use in the flight envelope protection systems since they provide a significant lead estimate [14]. It would be wrong to declare a method to be more efficient than another one before applying all methods to the same problem and comparing their performances. In this thesis, the neural-network based algorithms were chosen because in addition to their capability in the lead estimation, in the literature it is claimed that the neural network's ability to model a wide class of systems in many applications reduces the development time. Additionally, it offers better performance than the conventional techniques like PID-controllers provide.[22]

The developed neural network in this study is a three-layer feed-forward network. The first two layers use hyperbolic tangent basis functions and a linear basis function is used for the third layer. 8 neurons for the first layer, 6 neurons for the second layer, and one neuron for the third layer are used for the neural network structure. Levenberg-Marquardt back-propagation algorithm is used for training the network. To train the neural network, MATLAB software is used.[23] The obtained dynamic trim database is used for the training of the neural network. Figure 2.2.10 is the steady-state response of the trained neural network. The estimated and the actual rotor speed trim values at the same condition are shown.

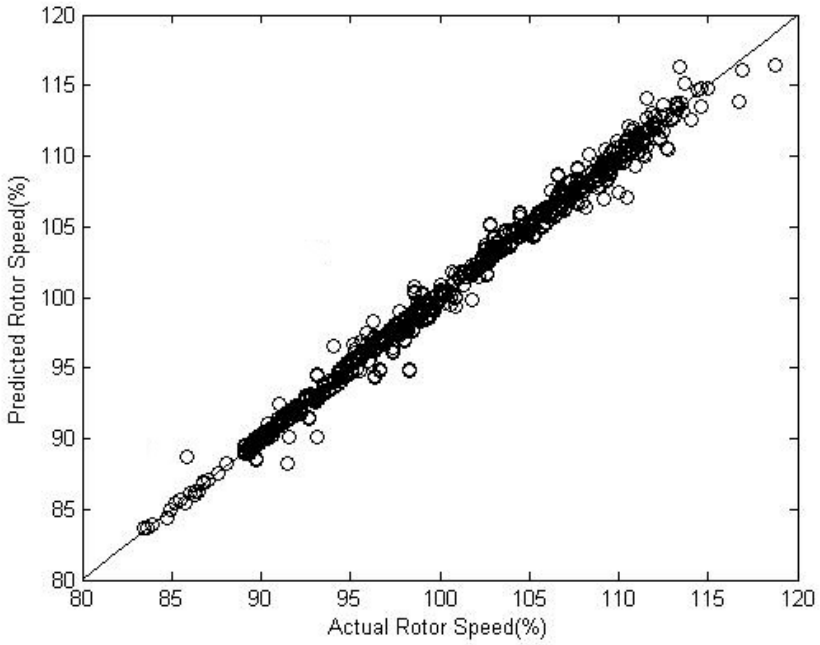

Figure 2.2.10 Neural network approximation of steady-state rotor speed

A dynamic test is performed in real-time to see the performance of the neural network in autorotation. For this test, a pitch angle reference is given to the helicopter model. The neural network is implemented into the helicopter simulation and the helicopter states and control inputs are connected to the neural network as inputs. A pilot model is used for the simulation which has vertical, longitudinal, lateral, and directional controllers. The lateral and directional channel controllers maintain the roll angle and heading at the trim state. The collective is fixed at the trim point. The longitudinal controller is following the pitch angle reference. The actual rotor speed of the helicopter model is compared with the predicted rotor speed resulting in a prediction error. This error is solved by implementing the correction proposed in [14], shown in Figure 2.2.11. The predicted rotor speed is passed through a low pass filter, then the error between this signal and actual rotor speed is added to the predicted rotor speed as a correction. The final dynamic response of the neural approximation and helicopter model is shown in Figure 2.2.13, for a given pitch angle reference signal, Figure 2.2.12. The reference is given while the helicopter is in autorotation with 65 knots forward speed, 1500 ft/min downward vertical speed at 4000ft altitude.

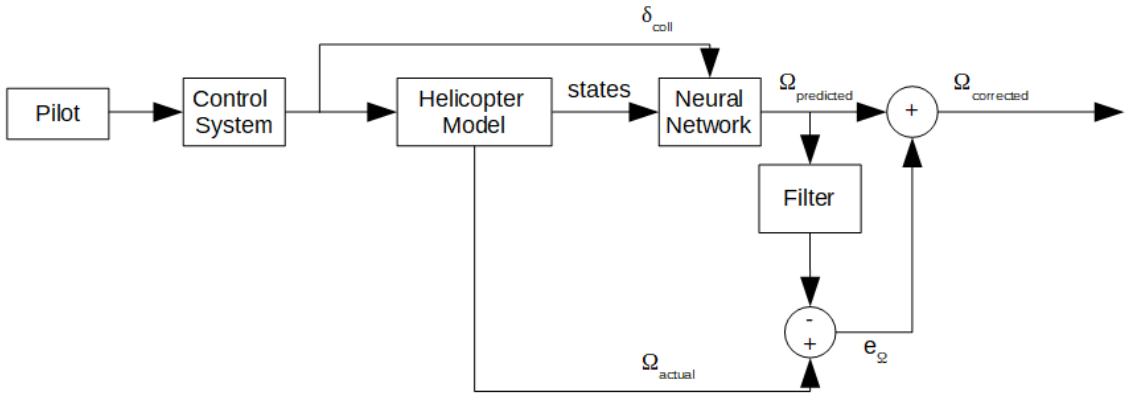

Figure 2.2. 11 Schematic representation of rotor speed estimation correction algorithm

The result shows that the neural network algorithm lead estimates the rotor speed which can be used to predict the rotor speed before it reaches the limit boundary.

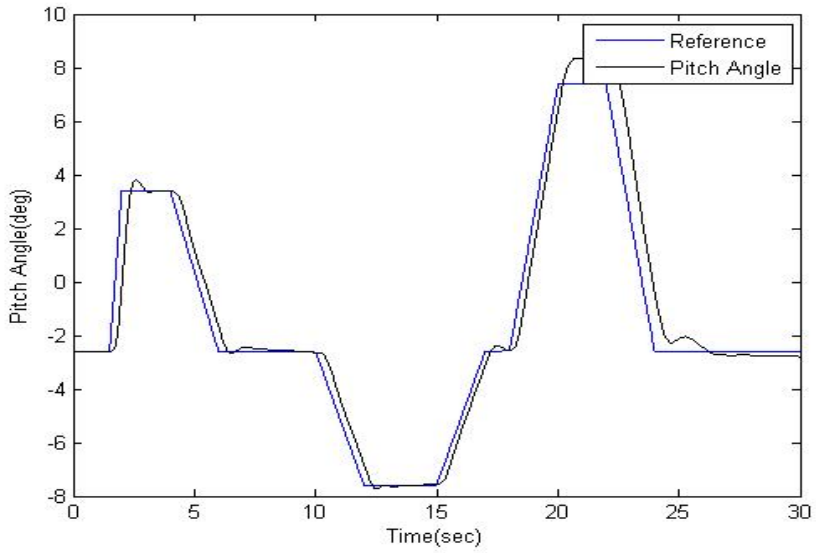

Figure 2.2.12 Maneuver, Pitch reference and pitch response of the helicopter in autorotation

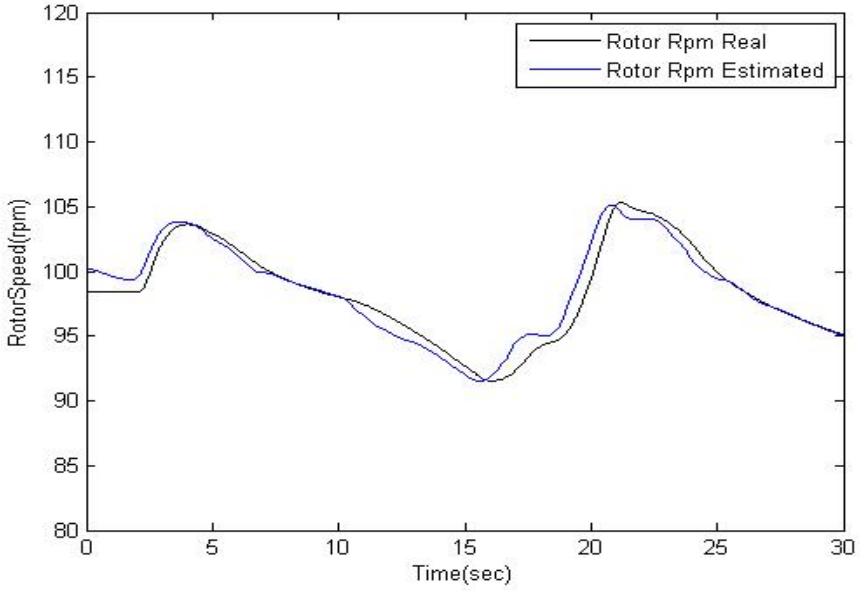

Figure 2.2.13 Neural network estimation and actual rotor speed

Comparing the neural network performance with the studies in the literature (Fig 1.2.13) shows that this model can be used for the lead estimation of the limit parameter.

2.3.Limit Protection

2.3.1. Limit Margin Estimation

For calculating the limit and control margins, it is required to linearize the neural network model[14]. The general open-loop equations of motion of the aircraft can be represented by a set of nonlinear state equations:

$$\dot{\boldsymbol{x}} = g(\boldsymbol{x}, \boldsymbol{u}) \tag{2.3.1}$$

where x is the states vector, and u is the input vector. For the calculation of the limit margin, the limit parameter must be defined. A vector of limited parameters can also be defined by a nonlinear function:

$$y_p = h(\boldsymbol{x}, \boldsymbol{u}) \tag{2.3.2}$$

In this study, the rpm response was chosen as the limited parameter and it was modeled as a function of known inputs and measured states, giving the rotor speed response. The local hub velocities will be addressed as V_x, V_y, V_z instead of $V_{xhub}, V_{yhub}, V_{zhub}$ for clarity in the chapter from this point. Hence, the neural network mapping can be written as:

$$\Omega_{pred} = f(\sigma_{coll}, \theta, V_x, V_y, V_z) \tag{2.3.3}$$

This nonlinear function is linearized using the Taylor series expansion. The linearized Taylor series approximation of the rotor speed function can be written as:

$$\Omega_{pred} = \Omega_0\left(\sigma_{coll_0}, \theta_0, V_{x0}, V_{y0}, V_{z0}\right) + \frac{\partial f}{\partial \sigma_{coll}}\left(\sigma_{coll} - \sigma_{coll_0}\right) + \frac{\partial f}{\partial \theta}(\theta - \theta_0) + \frac{\partial f}{\partial V_x}(V_x - V_{x0}) + \frac{\partial f}{\partial V_y}\left(V_y - V_{y0}\right) + \frac{\partial f}{\partial V_z}(V_z - V_{z0}) \tag{2.3.4}$$

By modifying the approximation, the variations in the limited parameter may be represented as:

$$\Omega_{pred} - \Omega_0 = \frac{\partial f}{\partial \sigma_{coll}}(\Delta\sigma_{coll}) + \left(\frac{\partial f}{\partial \theta}\dot{\theta} + \frac{\partial f}{\partial V_x}\dot{V}_x + \frac{\partial f}{\partial V_y}\dot{V}_y + \frac{\partial f}{\partial V_z}\dot{V}_z\right)\Delta t \tag{2.3.5}$$

Since the interest is on the collective input and pitch angle, rearranging the approximation as [14],

$$\Delta\Omega \approx \frac{\partial f}{\partial \sigma_{coll}}\Delta\sigma_{coll} + \frac{\partial f}{\partial \theta}\Delta\theta + \dot{\Omega}\Delta t \tag{2.3.6}$$

Hence, the control input margin and limit margin for the rotor speed can be approximated by,

$$\frac{\partial f}{\partial \sigma_{coll}}\Delta\sigma_{coll} + \frac{\partial f}{\partial \theta}\Delta\theta \approx \Delta\Omega - \dot{\Omega}\Delta t \tag{2.3.7}$$

Using a vector form

$$\begin{bmatrix} \frac{\partial f}{\partial \sigma_{coll}} & \frac{\partial f}{\partial \theta} \end{bmatrix} \begin{bmatrix} \Delta\sigma_{coll} \\ \Delta\theta \end{bmatrix} \approx \Delta\Omega - \dot{\Omega}\Delta t \tag{2.3.8}$$

The critical control margin is the difference between the current control position and the related limit boundary. Likewise, the critical limit margin is the difference between the current pitch angle and its value at the related limit boundary. This can be calculated by taking the inverse of the partial derivative matrix:

$$\begin{bmatrix} \Delta\sigma_{coll} \\ \Delta\theta \end{bmatrix} \approx \left(\Delta\Omega - \dot{\Omega}\Delta t\right) \begin{bmatrix} \frac{\frac{\partial f}{\partial \sigma_{coll}}}{\left(\frac{\partial f}{\partial \sigma_{coll}}\right)^2 + \left(\frac{\partial f}{\partial \theta}\right)^2} \\ \frac{\frac{\partial f}{\partial \theta}}{\left(\frac{\partial f}{\partial \sigma_{coll}}\right)^2 + \left(\frac{\partial f}{\partial \theta}\right)^2} \end{bmatrix} \tag{2.3.9}$$

$\Delta\Omega$ represents the difference between the value of the rotor speed at the limit boundary and its current value. Δt is an arbitrary time margin that can be selected ensuring the limit is not exceeded. The partial derivative terms represent the sensitivity of the neural network model output to the given control inputs. They are calculated by perturbing the network model at several trim points. The selected points around which the linearization is performed were selected from the dynamic trim database previously generated to model the neural network. By giving perturbations for collective control and pitch angle, the partial derivatives were calculated around each trim point.

Since the rotor rpm was found to be a fast state for pitch angle and collective input, margins for this parameter and control input are used for the limit protection.

2.3.2. Limit Protection Algorithm

As explained in Chapter 1, pilot cueing can be done using several methods. In order to not exceed rotor speed boundaries in autorotation, it is important to stay inside the available pitch angle margin and collective input margin. To cue the pilot with pitch angle limits during autorotative flight, the limit can be indicated on the displays. This way, the pilot can track the helicopter pitch angle and fix it if necessary with the longitudinal cyclic inputs to stay inside safe boundaries.

This pitch limit margin cue is simulated in this study such that the pitch angle reference given to the pilot model is saturated with calculated upper and lower pitch angle margins. The pilot model will try to track the saturated reference as if in real flight the pilot is avoiding the pitch angle limits. The pitch angle limit avoidance algorithm is shown schematically in Figure 2.3.1.

For the collective control limit cueing in a real piloted helicopter, methods like tactile cueing can be used. In this thesis, the collective cue will be assumed as a hard stop. The calculated control margin will be used to saturate the pilot model collective input. The inputs above or below the margin will not be allowed. This control limiting algorithm is shown schematically in Figure 2.3.2.

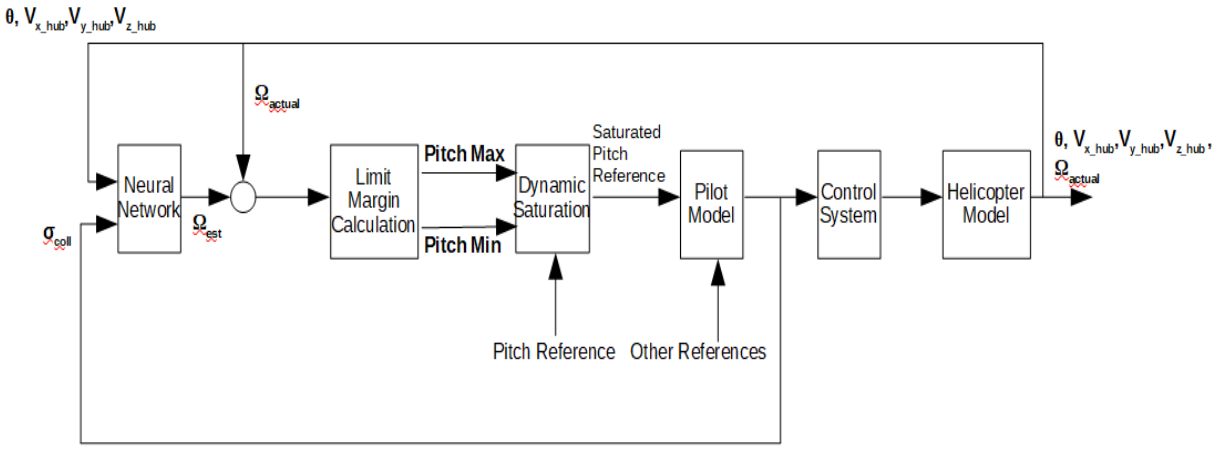

Figure 2.3.1 Schematic representation of avoiding calculated pitch angle limit margin

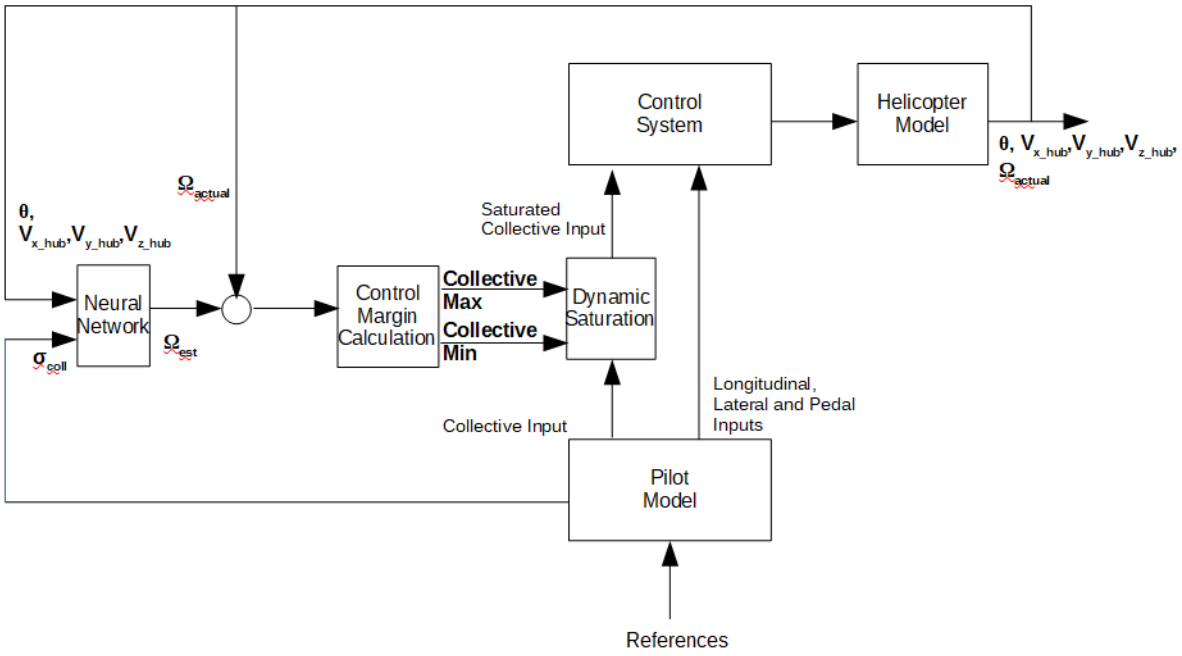

Figure 2.3.2 Schematic representation of collective control limiting flight envelope protection

3. RESULTS AND DISCUSSION

The results of the thesis study are presented in two categories. Firstly, simulation results for the envelope protection using pitch angle parameter cueing are presented. Secondly, simulation results for the envelope protection using collective control input cueing are presented.

3.1. Pitch angle as a limit parameter

For the pitch angle limit parameter, three maneuvers were defined to investigate the protection system. A smooth pitch-up reference, a smooth pitch-down reference, and an aggressive pitch up and down reference are introduced to the pilot model. The pilot model tracks the given pitch angle reference with the longitudinal cyclic. The roll angle and heading are kept at the trim state by the pilot model using the lateral cyclic and pedal inputs. The collective input tracks the given vertical speed reference. The high and low rotor rpm limits are 110% and 90%. These are the safe boundary limits during autorotation.

3.1.1. Case 1: Smooth Pitch Up Maneuver

First, the helicopter is trimmed at a steady-state autorotation point where the rotor speed is close to the high rotor rpm limit. The trim point is at 6000ft height, the helicopter is trimmed at a 95 knots airspeed and -3800 ft/min vertical speed autorotation. A smooth pitch up reference is given. The vertical speed at the trim state is given as a reference to the pilot model. The simulation results without using the protection system are shown in Figure 3.1.1. and 3.1.2.

In Fig 3.1.1 the first plot shows the rotor speed (Ω) response. The blue line represents the rotor speed estimation of the neural network model. The black line represents the actual helicopter model response. The dashed red lines represent the high and low rpm limits that the helicopter should not exceed. The second plot shows the helicopter pitch angle (θ) response represented with a black solid line. The black dashed line is the given pitch

angle reference. Since the reference is given smoothly and the delta pitch reference is small, the pilot model tracks the reference successively. The dashed red lines are the calculated pitch angle limit margins. The margins are calculated at each time step and they change with the changing helicopter states and control inputs. As can be seen from the figure, the pitch angle limit margin is exceeded when the rotor speed limit is exceeded.

In Fig 3.1.2 the first and second plots show the corresponding longitudinal cyclic input (σ_{long}) and the collective input (σ_{coll}), respectively. The final plot shows the vertical speed response of the helicopter. Since the collective is already at a full-down position (0%), the pilot model can not keep the vertical speed at the trim value when the helicopter nose up maneuver decreases the descent rate. Hence the collective input is constant. The pilot inputs are saturated at the limits of the control system so that the inputs are not unrealistic. For example, the collective input mapping is from 0 to 100% and collective input can not go above 100% or below 0% in this case.

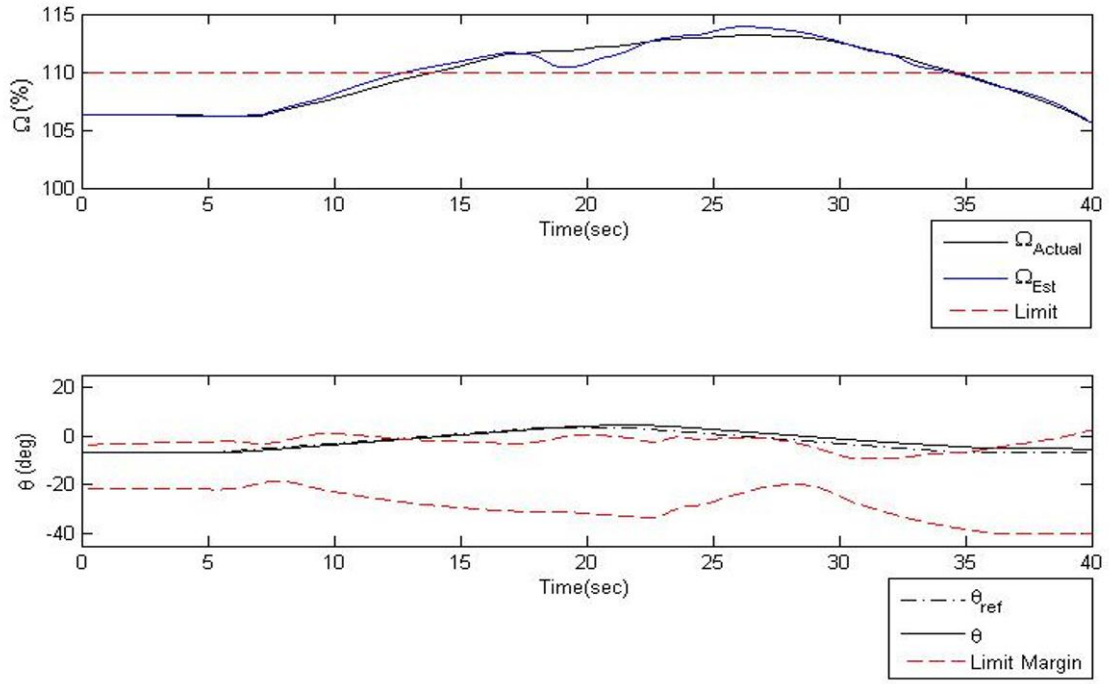

Figure 3.1.1 Smooth pitch up maneuver rotor speed and pitch angle response, without envelope protection

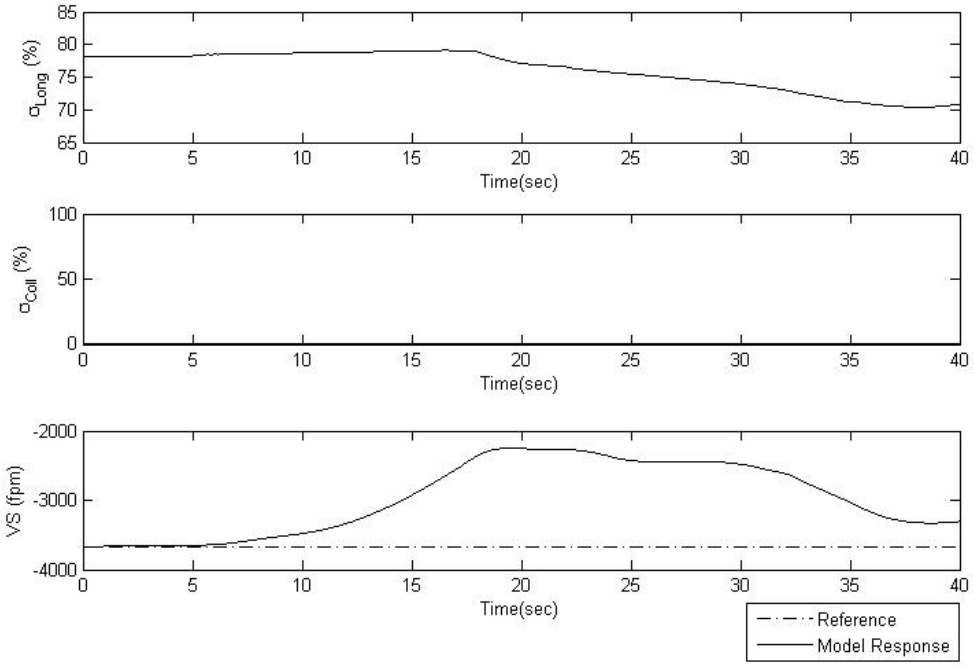

Figure 3.1.2 Smooth pitch up maneuver control inputs and vertical speed response, without envelope protection

The same pitch up maneuver is performed using the envelope protection system. Figure 3.1.3 and 3.1.4 show the helicopter responses and control inputs when the envelope protection is used. The solid black lines represent the helicopter model responses, the dashed black lines represent the given references, and the red dashed lines represent the limits. As can be seen from the figure, the given pitch angle reference was saturated using the calculated limit margin. The pilot model tracked the saturated pitch angle reference. This prevented the rotor speed limit exceedance successfully.

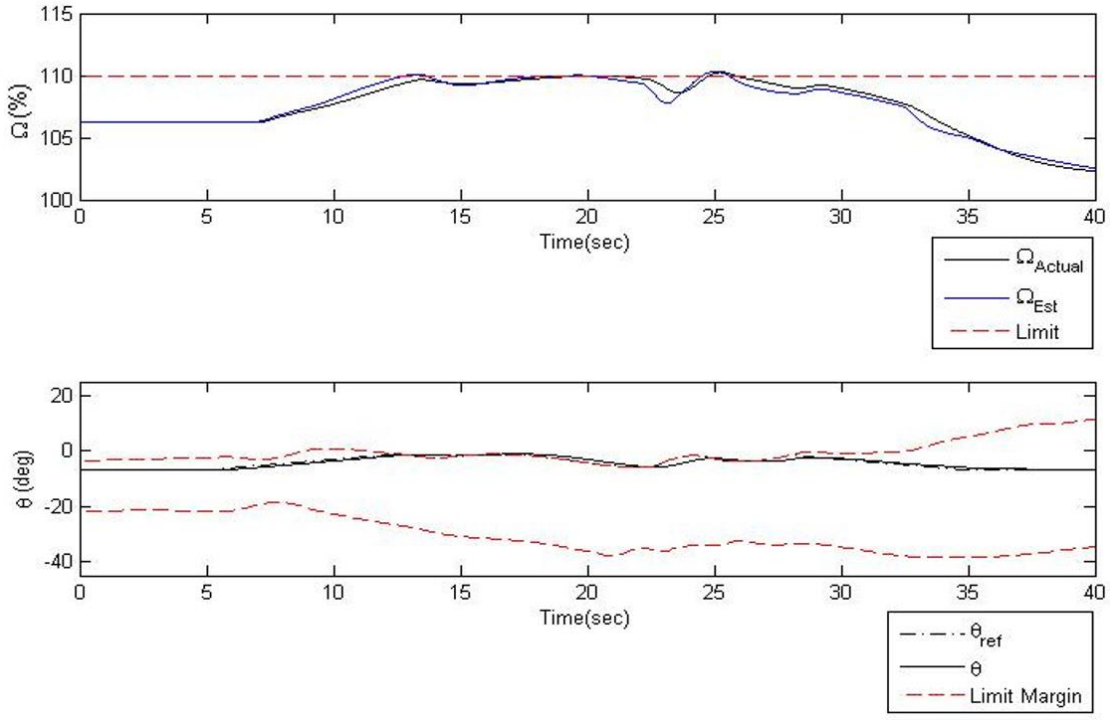

Figure 3.1.3 Smooth pitch up maneuver rotor speed and pitch angle response, with envelope protection

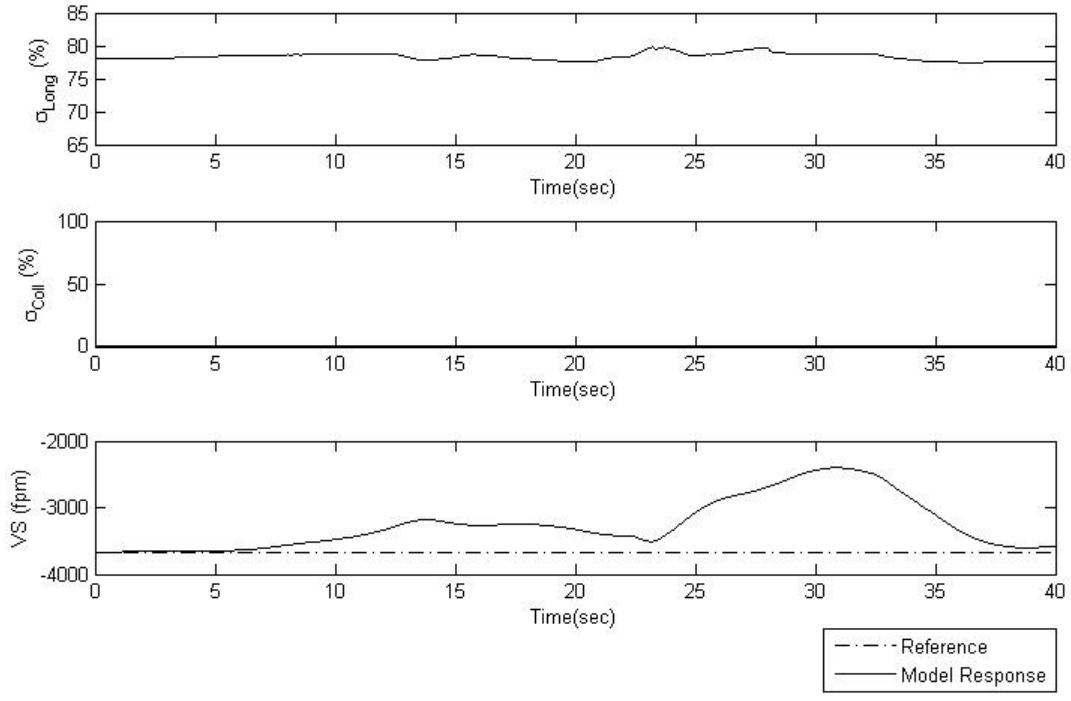

Figure 3.1.4 Smooth pitch up maneuver control inputs and vertical speed response, without envelope protection

This maneuver shows that even small amounts of pitch angle change may cause the rotor rpm to exceed its limits. The envelope protection system using the calculated pitch angle margins successfully prevented the rotor rpm to exceed the high rpm limit.

3.1.2. Case 2: Smooth Pitch Down Maneuver

The same procedure is performed for a pitch down maneuver to see the effect of the envelope protection system when the rotor speed decreases below the low rotor rpm limit. The helicopter was trimmed at 4000ft altitude, 65 knots airspeed, and -1500ft/min vertical speed. A smooth pitch down reference was given to the pilot model.

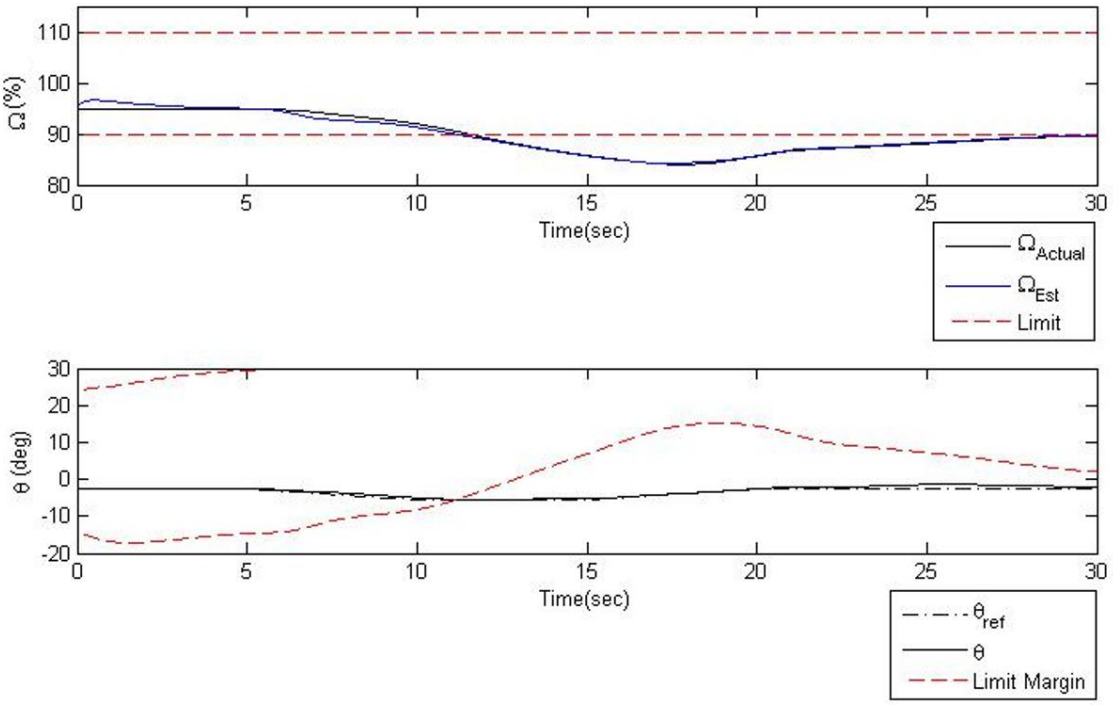

Figure 3.1.5 Smooth pitch down maneuver, rotor speed, and pitch angle response, without envelope protection

Figure 3.1.5 shows the rotor speed response and pitch angle response. The calculated pitch angle margin is zero when the estimated rotor speed exceeds the low rotor rpm limit. Since the reference change is given very slowly, the estimation lead time is very small compared to an aggressive input. Since the reference changes slowly, the time difference

between the convergence of the fast and slow states decreases. Still, the estimation is enough to calculate a pitch margin and can be used for envelope protection.

Figure 3.1.6 shows the corresponding longitudinal and collective inputs, and the vertical speed response of the helicopter.

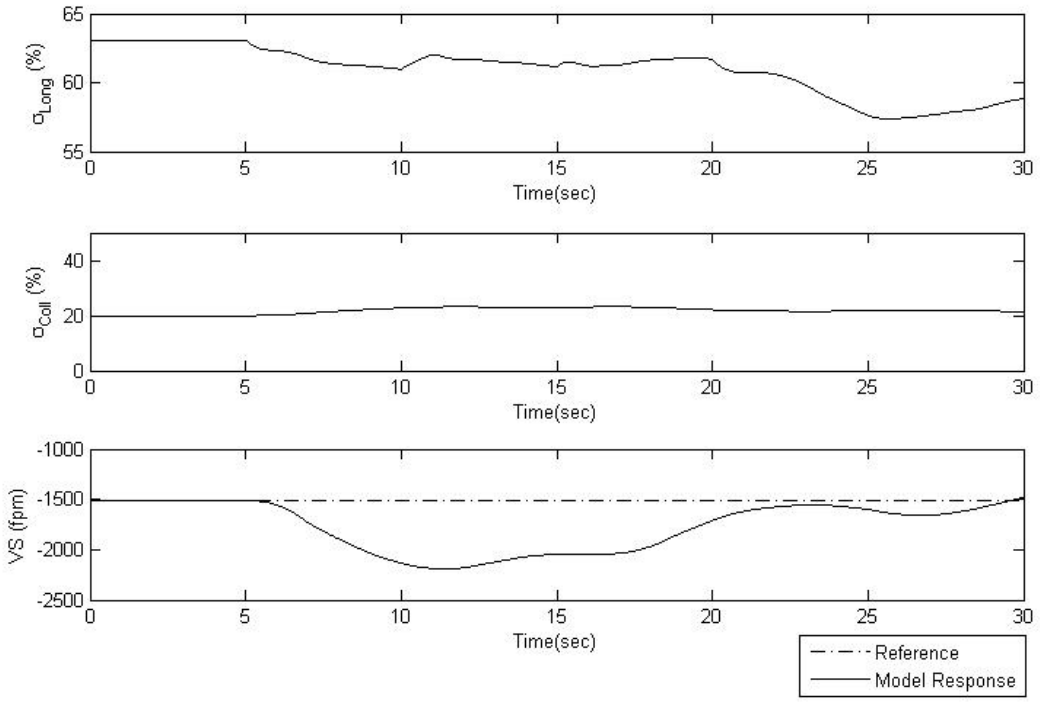

Figure 3.1.6 Smooth pitch down maneuver, control inputs, and vertical speed response, without envelope protection

The same pitch down maneuver was repeated by saturating the pitch angle reference with the calculated limit margins. Figure 3.1.7 shows the rotor rpm response and the saturated pitch angle. Figure 3.1.8 shows the control inputs and vertical speed response.

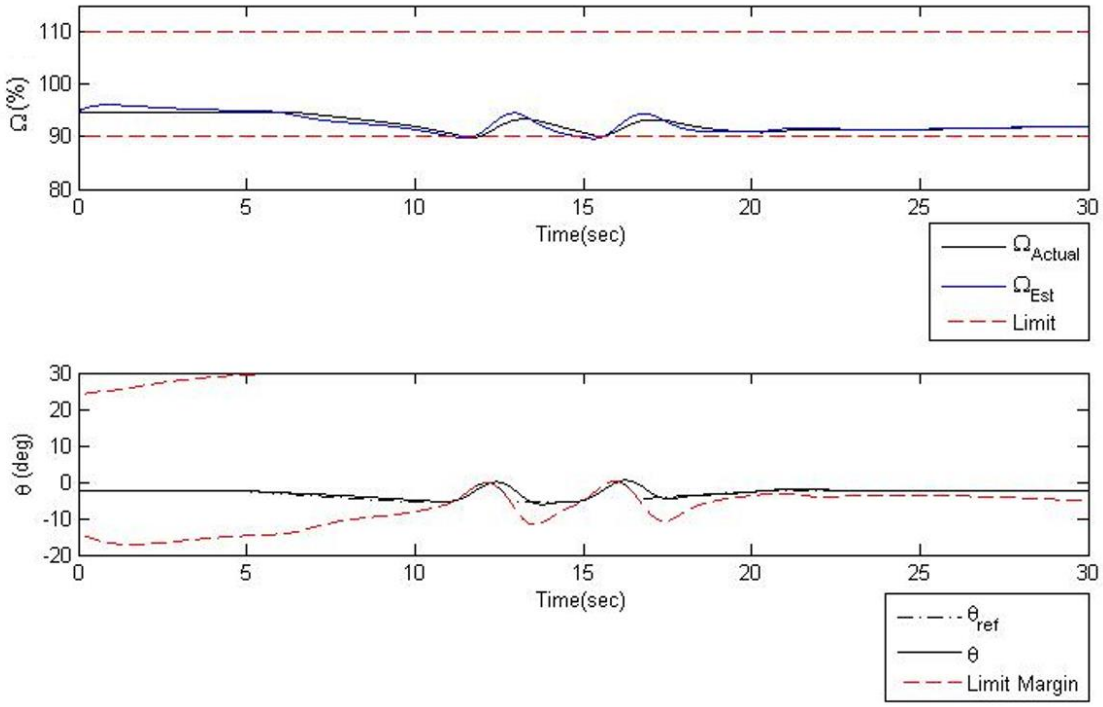

Figure 3.1.7 Smooth pitch down maneuver, rotor speed, and pitch angle response, with envelope protection

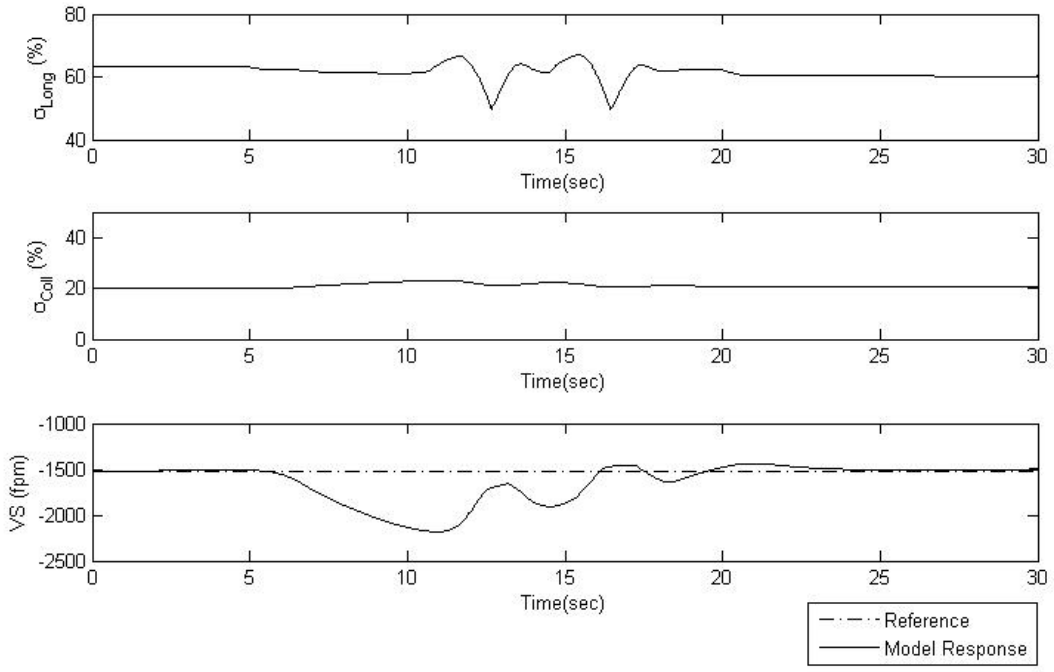

Figure 3.1.8 Smooth pitch down maneuver, control inputs, and vertical speed response, with envelope protection

The results show that for smooth pitch maneuvers, the developed flight envelope protection system using pitch angle as a limit parameter effectively works to prevent the rotor speed limit exceedance.

3.1.3. Case 3: Aggressive Pitch Up and Down Maneuver

To investigate the effectiveness of the developed system, a more aggressive pitch maneuver is performed with the pilot model. The rotor rpm responses were compared with and without the envelope protection system.

A sudden pitch up reference and then a steep pitch down reference were given to the pilot model as shown in Figure 3.1.9. As a result, the rotor speed went above the high rotor rpm limit first, and then it went below the low rotor rpm limit, also shown in Figure 3.1.9. The corresponding control inputs and vertical speed response of the maneuver are shown in Figure 3.1.10. Due to the pitch down reference, the descent rate constantly increases. The vertical controller of the pilot model increases the collective to slow down the descent but this also contributes to the decrease of the rotor rpm.

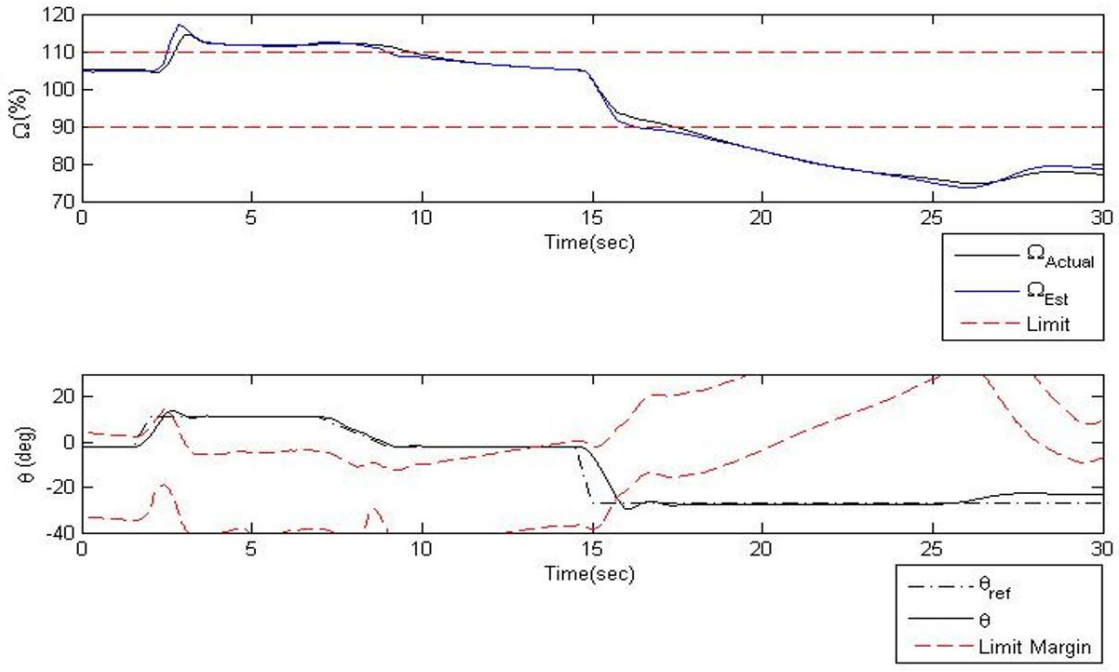

Figure 3.1.9 Aggressive pitch maneuver, rotor speed, and pitch angle response, without envelope protection

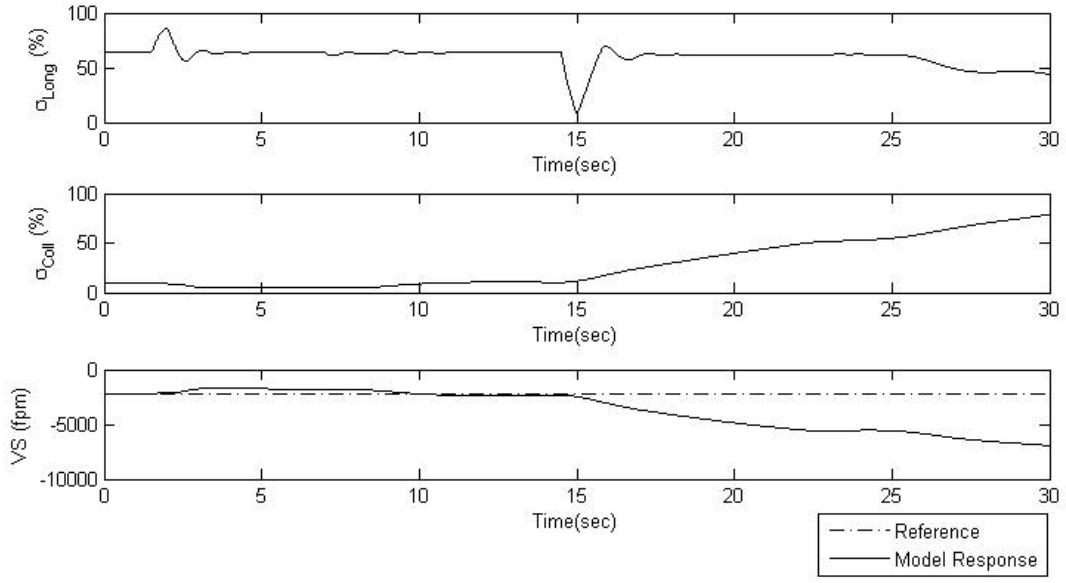

Figure 3.1.10 Aggressive pitch maneuver, control input, and vertical speed response, without envelope protection

The same aggressive maneuver was performed using the envelope protection system by saturating the pitch angle reference with the calculated limit margins. The rotor speed and pitch angle responses are shown in Fig 3.1.11. The corresponding control inputs and vertical speed response are shown in Fig 3.1.12.

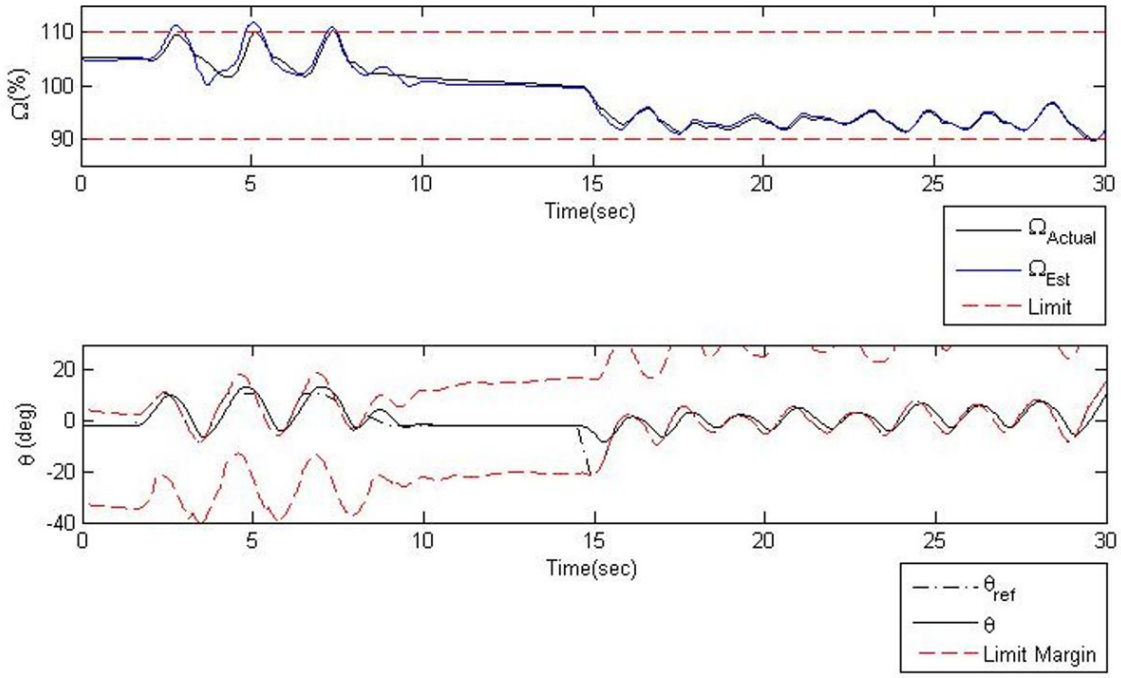

Figure 3.1.11 Aggressive pitch maneuver, rotor speed, and pitch angle response, with envelope protection

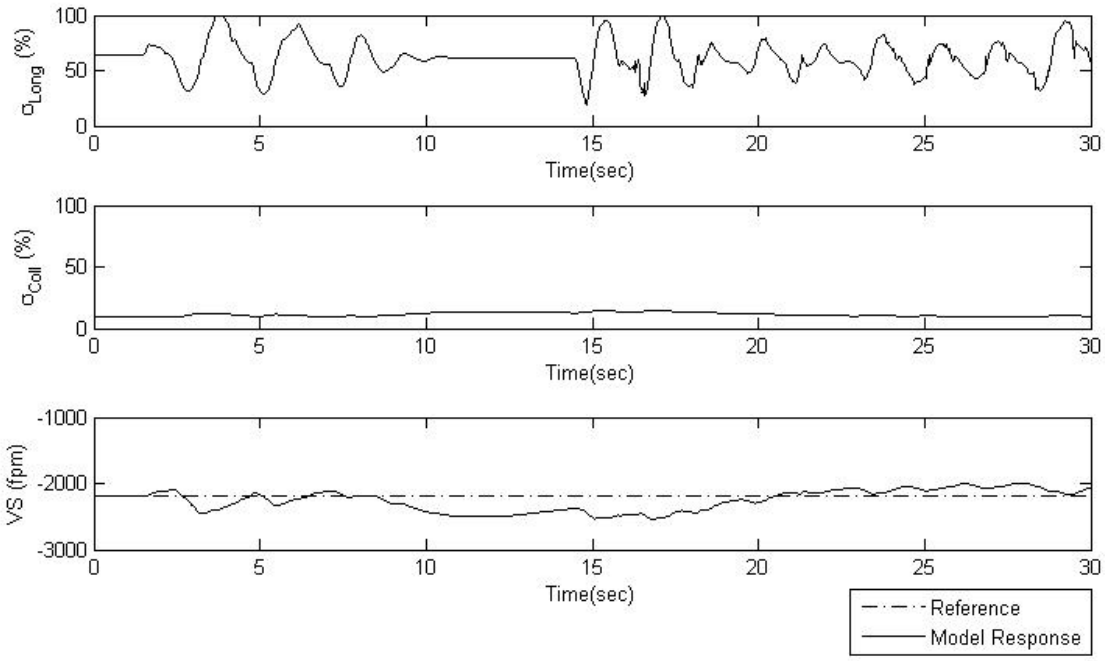

Figure 3.1.12 Aggressive pitch maneuver, control inputs, and vertical speed response, with envelope protection

3.2. Collective Input as a Control Limit

As explained in Chapter 2, a collective cue is also calculated for envelope protection. Two cases were performed for the collective control margin. For these maneuvers, both pitch angle and vertical speed references were given to the pilot model at the same time. The control margins for the collective control were calculated. The collective control input was saturated using these calculated margins.

3.2.1. Case 4: High Rotor rpm Limit Exceedance

The helicopter was trimmed at 2000 ft height, 65 knots airspeed, and -1600 ft/min vertical speed. A pitch up reference together with an increase in descent rate were given as a reference to the pilot model. Figure 3.2.1 shows the longitudinal cyclic input, the pitch angle reference and response, and the vertical speed reference and the response of the helicopter.

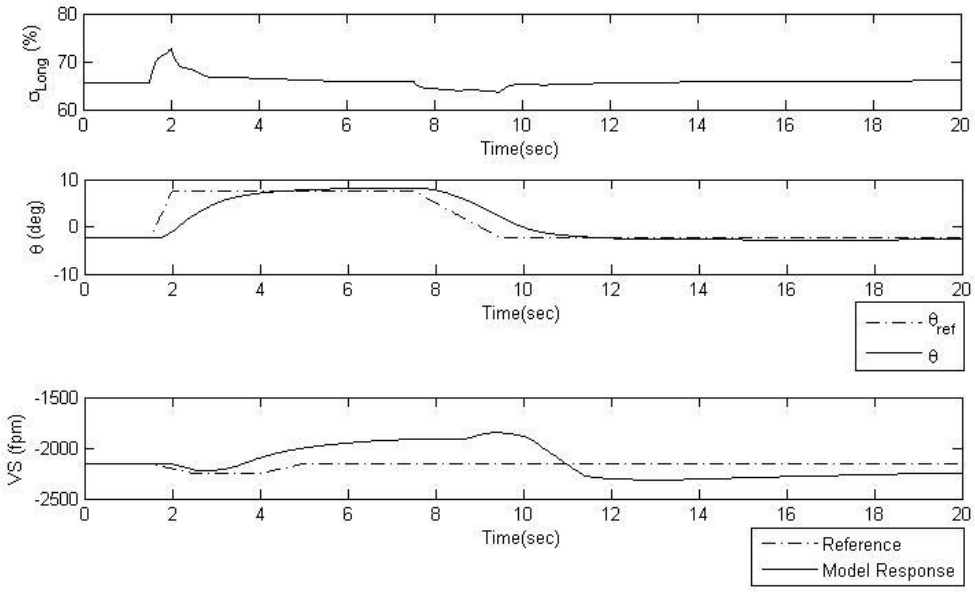

Figure 3.2.1 Pitch up maneuver, pilot model references, and corresponding longitudinal input, without envelope protection

The corresponding rotor speed response and the collective control input are shown in Figure 3.2.2. As can be seen from the results, the high rotor speed limit is exceeded by performing this maneuver without using the envelope protection system.

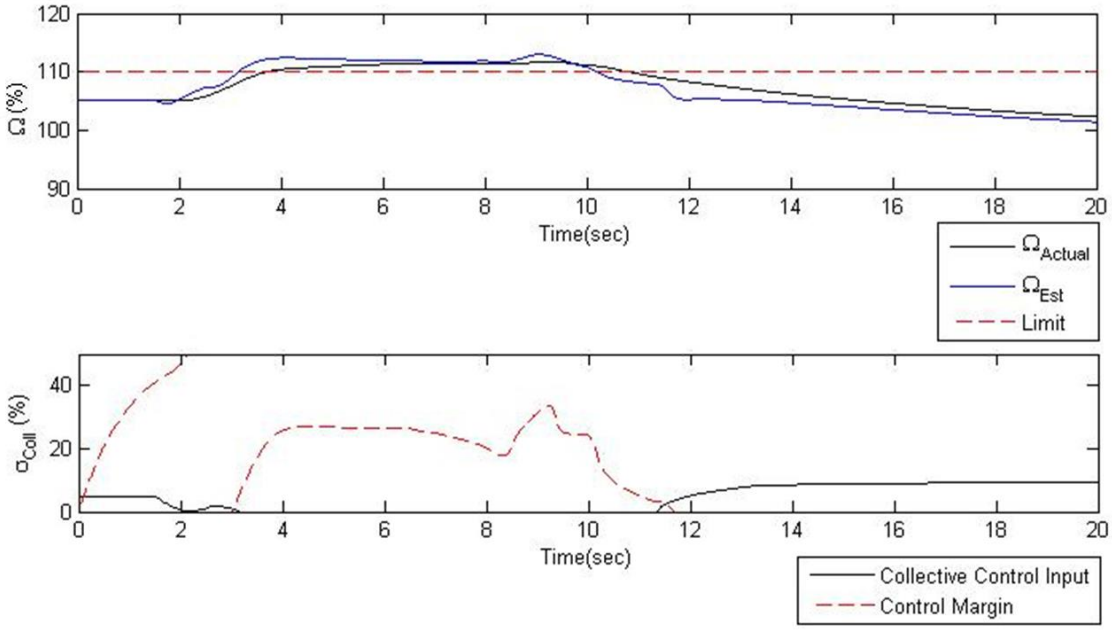

Figure 3.2.2 Pitch up maneuver, rotor speed response, and collective control input, without envelope protection

The same maneuver was performed by saturating the collective control input using the calculated control margins. Figure 3.2.3 shows the longitudinal cyclic input, the pitch angle response, and the vertical speed response. Figure 3.2.4 shows the rotor speed response and the saturated collective control input.

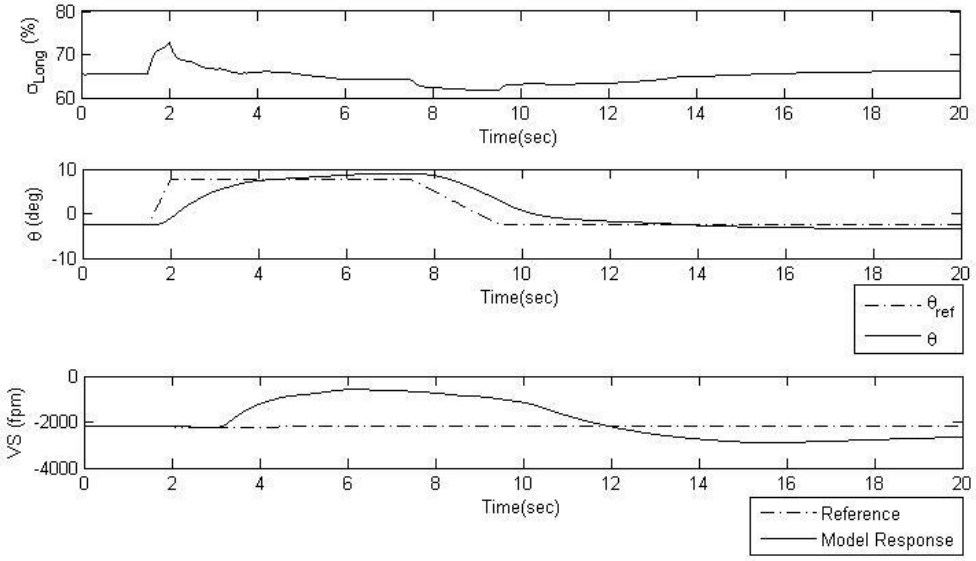

Figure 3.2.3 Pitch down maneuver, pilot model references, and corresponding longitudinal input, with envelope protection

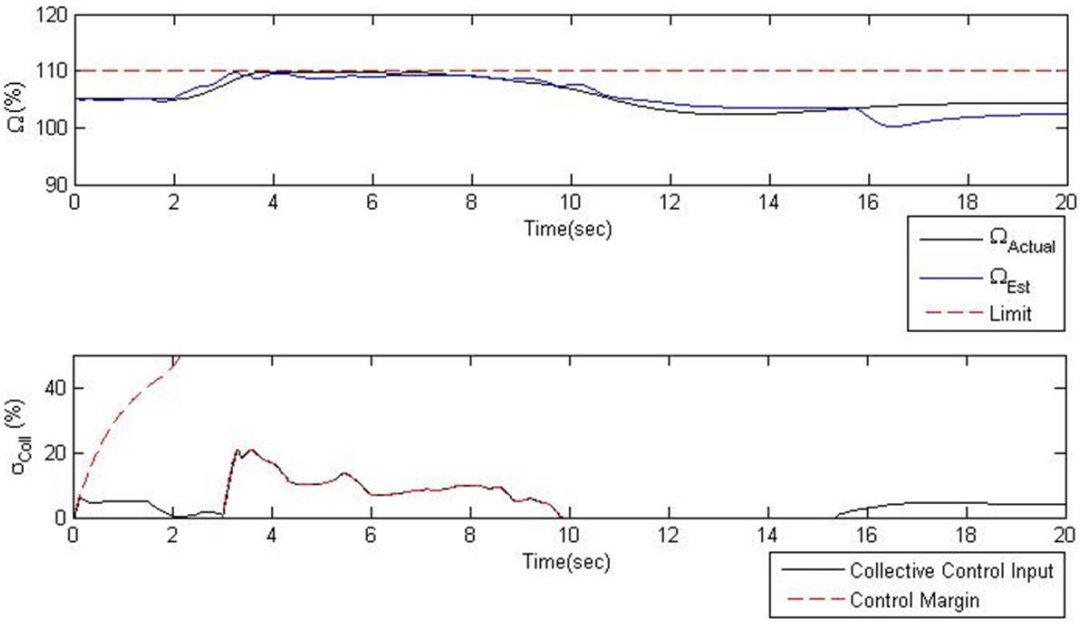

Figure 3.2.4 Pitch down maneuver, rotor speed response, and collective control input, with envelope protection

Using the control input saturation, the rotor speed limits were not exceeded and the rotor speed stayed inside the safe limits.

3.2.2. Case 5: Low Rotor rpm Limit Exceedance

For the fifth test case, a pitch angle and a vertical speed reference were given to the pilot model at the same time. Pitch down maneuver is performed while decreasing the descent rate.

Figure 3.2.5 shows the rotor rpm response and the collective control input of the pilot model. As can be seen from the figure, the estimated rotor rpm decreases below the low rpm limit, and the calculated collective control margin is also exceeded. Figure 3.2.6 shows the longitudinal cyclic input, pitch angle, and vertical speed responses and references.

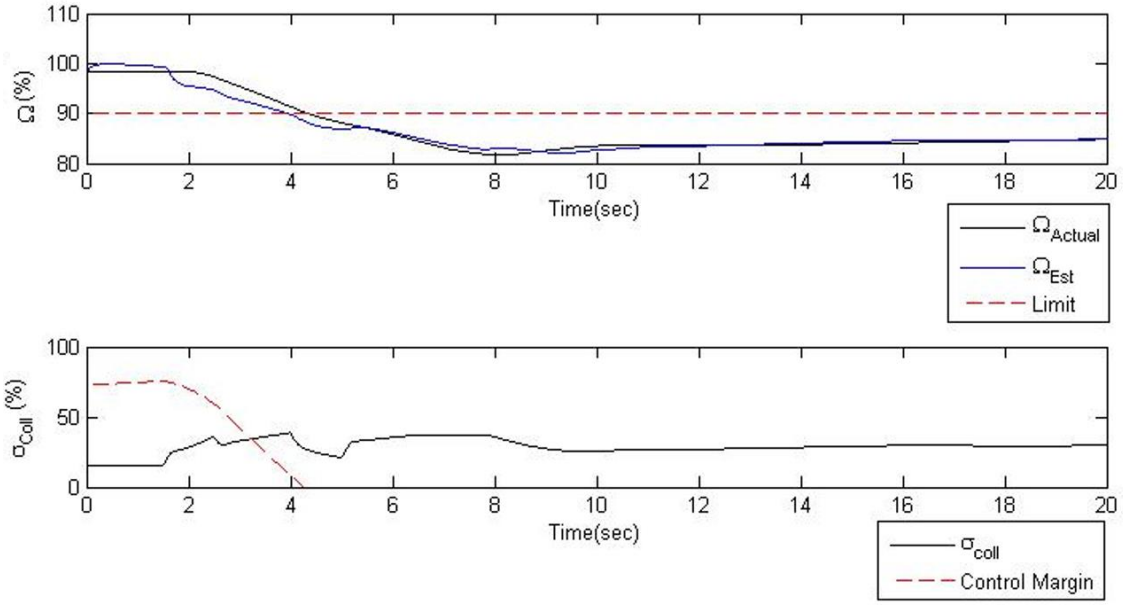

Figure 3.2.5 Pitch down maneuver, rotor speed response, and collective control input, without envelope protection

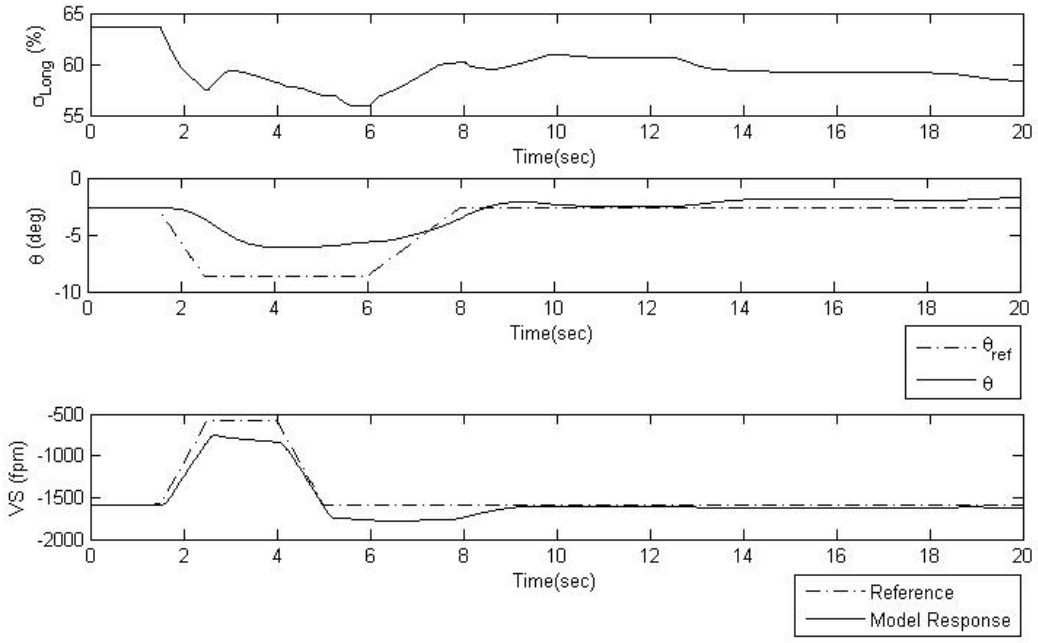

Figure 3.2.6 Pitch down maneuver, pilot model references, and corresponding longitudinal input, without envelope protection

The same maneuver was repeated using the envelope protection system which saturates the pilot's collective input. Figure 3.2.7 shows the rotor speed response which does not exceed the limit and the saturated collective input. Figure 3.2.8 shows the longitudinal cyclic input, pitch angle, and vertical speed responses of the helicopter during the maneuver.

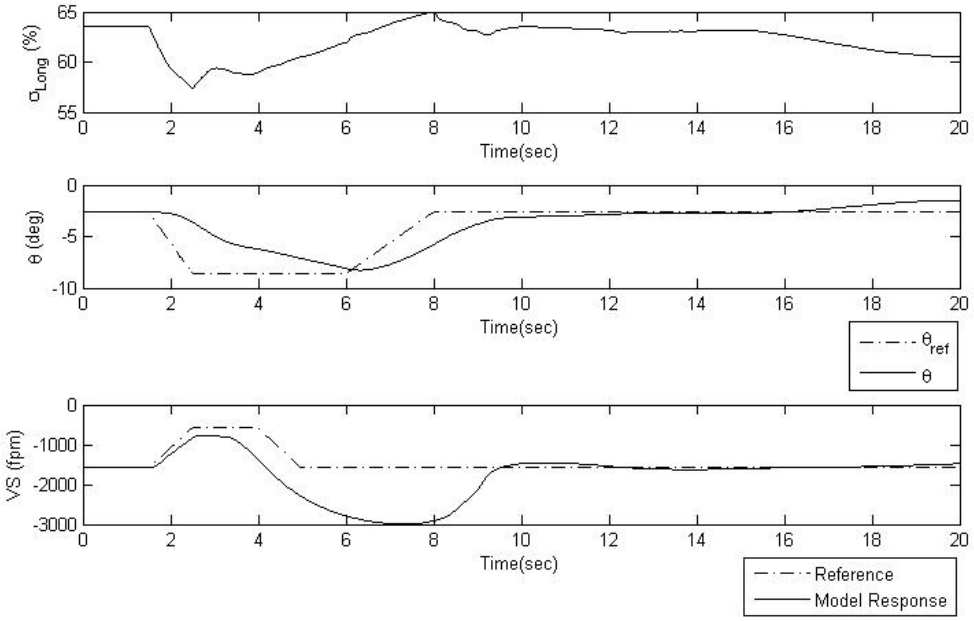

Figure 3.2.7 Pitch down maneuver, pilot model references, and corresponding longitudinal input, with envelope protection

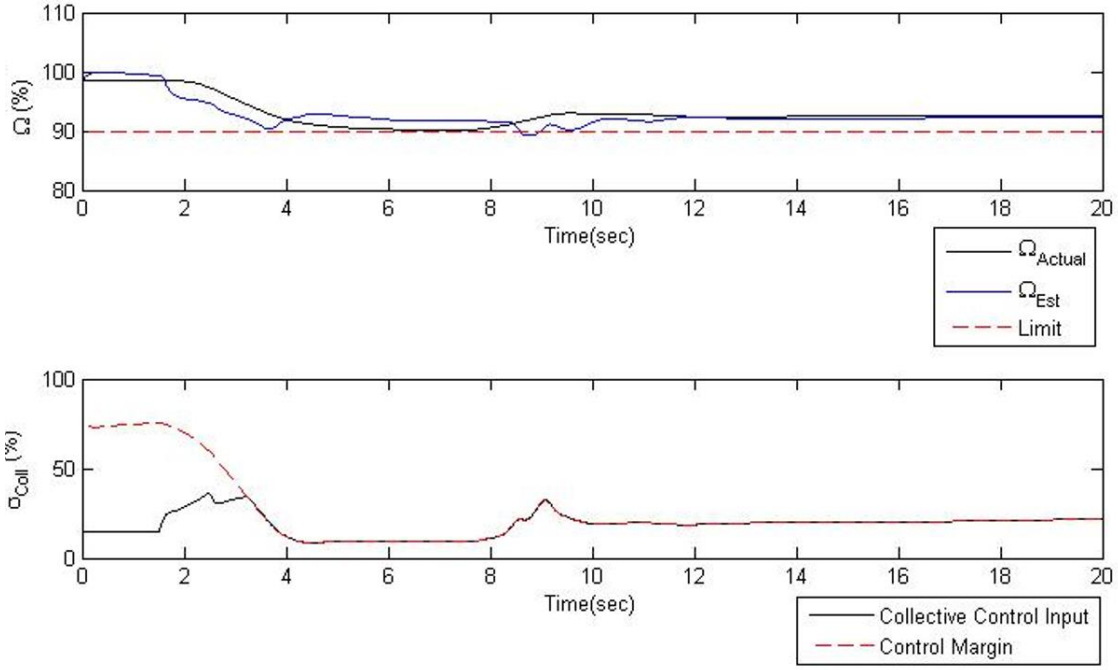

Figure 3.2.8 Pitch down maneuver, rotor speed response, and collective control input, with envelope protection

4. CONCLUSION

In this thesis, a rotor speed estimation model was developed using a neural network based algorithm for a helicopter at autorotation. The estimation model is based on collective input, helicopter pitch angle, and the local hub velocities. This estimation model is used to predict the limit exceedance. Using the lead estimate, the collective input margin and pitch angle margin are calculated. Two flight envelope protection methodologies were proposed using these margins. Simulations were presented with a developed helicopter model. In these simulations, different maneuvers were performed at several autorotation flight conditions. The envelope protection strategies were shown to be successful in preventing the rotor speed limit exceedance.

During the development of the estimation model, the rotor speed behavior was investigated. Note that in the literature, the estimation models are generally based on control inputs. It is known that during autorotation, the pilots control the rotor speed with the longitudinal motion of the helicopter as well as the collective input. But for a given longitudinal cyclic step input, the helicopter does not converge to a trim state. Therefore, the effect of pitch angle change on rotor speed was investigated. The rotor speed was observed to be fast-responsive to a helicopter pitch angle change and a given collective input.

The developed neural network algorithm was trained offline. A further improvement of this study may be training this network online using an adaptive neural network. But, since this system is developed only for autorotation, the flight regime is restricted. The database that should be used for training is not as big as a full flight envelope condition. The conditions are limited. The trim condition database was generated for different weights, different airspeeds, at different altitudes, and vertical speeds. These variables are limited compared to a full flight scenario. Hence, offline training of the neural network was found to be sufficient.

The calculated pitch angle margin and collective control margin can be used to cue the pilot during a piloted flight. In this study, since the demonstration is performed in

a simulation environment, a pilot model is developed to perform some maneuvers. In real life, these margins can be cued to the pilot with different methods. The two proposed methods can be used separately, as well as together at the same time. To integrate the two methods a weighting system can be developed as a further improvement to the study. Some algorithms can be developed to decide which margin should be used at which conditions. In this study, the methods are used separately. The pitch margin cueing was assumed to be shown in the pitch angle display, and it was assumed that the pilot model tracks the pitch angle margin while performing another maneuver, keeping the pitch angle inside the margins which results in preventing the rotor speed limit exceedance. Another future research would be mapping the pitch angle margin to the longitudinal cyclic control and preventing the inputs that would cause the helicopter to exceed the calculated pitch angle margin. This could be done using tactile cueing or by manipulating the pilot inputs at the AFCS. The collective input margin can also be used in the same manner.

5. REFERENCES

[1] International Virtual Aviation Organisation, “Helicopter Main Flight Controls.” https://mediawiki.ivao.aero/index.php?title=Helicopter_flight_controls_introduction.

[2] Federal Aviation Administration, “Helicopter flight controls,” 2009. https://www.faasafety.gov/gslac/ALC/course_content.aspx?cID=105&sID=456&preview=true.

[3] W. Johnson, *Helicopter Theory*. New York: Dover Publications, Inc., 1946.

[4] M. E. Dreier, *Introduction to Helicopter and Tiltrotor Flight Simulation*, 1st ed. Reston: American Institute of Aeronautics and Astronautics, Inc., 2007.

[5] G. Gratton, *Initial airworthiness: Determining the acceptability of new airborne systems: Second edition*. Springer International Publishing Switzerland, 2018.

[6] J. R. Mayo and V. N. Iannacci, “The RAH-66 Comanche Flight Envelope Cueing System,” 1999.

[7] K. A. Ackerman *et al.*, “Automation situation awareness display for a flight envelope protection system,” *J. Guid. Control. Dyn.*, vol. 40, no. 4, pp. 964–980, 2017, doi: 10.2514/1.G000338.

[8] V. Sahasrabudhe, J. F. Horn, N. Sahani, A. Faynberg, and R. Spaulding, “Simulation investigation of a comprehensive collective-axis tactile cueing system,” *J. Am. Helicopter Soc.*, vol. 51, no. 3, pp. 215–224, 2006, doi: 10.4050/1.3092883.

[9] M. Whalley, W. Hindson, G. Thiers, and M. Rutkowski, “A Comparison of Active Sidestick and Conventional Inceptors for Helicopter Flight Envelope Tactile Cueing,” 2000.

[10] A. J. D. Bateman, D. G. Ward, R. L. Barron, and M. S. Whalley, “Piloted simulation evaluation of a neural network limit avoidance system for rotorcraft,” *24th Atmos. Flight Mech. Conf.*, no. c, pp. 661–673, 1999, doi: 10.2514/6.1999-4252.

[11] L. Binet, A. Taghizad, M. Abildgaard, and W. Von Grunhagen, “VRS avoidance as active function on side-sticks,” *Annu. Forum Proc. - AHS Int.*, vol. 2, no. September 2017, pp. 1642–1660, 2009.

[12] W. Falkena, C. Borst, Q. P. Chu, and J. A. Mulder, “Investigation of practical flight envelope protection systems for small aircraft,” *J. Guid. Control. Dyn.*, vol. 34, no. 4, pp. 976–988, 2011, doi: 10.2514/1.53000.

[13] G. Gürsoy, “Direct Adaptive Flight Envelope Protection,” Middle East Technical University, 2016.

[14] J. F. Horn, A. J. Calise, and J. V. R. Prasad, “Flight envelope cueing on a tilt-rotor aircraft using neural network limit prediction,” *J. Am. Helicopter Soc.*, vol. 46, no. 1, pp. 23–31, 2001, doi: 10.4050/jahs.46.23.

[15] J. J. Howlett, “UH-60 A Black Hawk Engineering Simulation Model,” 1981.

[16] R. K. Heffley and M. A. Mnich, “Minimum Complexity Helicopter Simulation Math Model,” 1988.

[17] H. Glauert, “A General Theory of the Autogyro,” *Sci. Res. Air Minist. - Reports Memo. No. 1111*, p. 41, 1926.

[18] D. M. Pitt and D. A. Peters, “Theoretical Prediction of Dynamic-Inflow Derivatives.,” no. July, 1980.

[19] K. B. Hilbert, “A Mathematical Model of the UH-60 A Black Hawk,” *NASA Tech. Memo. 85890*, p. 39, 1984.

[20] A. R. S. Bramwell, G. Done, and D. Balmford, *Bramwell’s Helicopter Dynamics*, 2nd ed. Oxford: Butterworth-Heinemann, 2001.

[21] N. A. Sahani and J. F. Horn, “Neural network based algorithms for comprehensive collective axis limit avoidance on rotorcraft,” *J. Aerosp. Comput. Inf. Commun.*, vol. 1, no. NOV., pp. 432–451, 2004, doi: 10.2514/1.6259.

[22] O. Ravn, L. Hansen, N. Poulsen, and M. Norgaard, *Neural networks for modelling and control of dynamic systems*. London: Springer, 2000.

[23] H. Demuth and M. Beale, *Neural network*. The MathWorks, Inc., 1994.